CHEMICAL SYNTHESIS OF CNC NANOPARTICLES FROM LIGNOCELLULOSES AND THEIR APPLICATION IN WASTE WATER TREATMENT

Thesis submitted in partial fulfilment of the requirements for awards of the degree of Master of Engineering in Bioprocess Engineering

Submitted by

DEBALINA MONDAL

Class Roll No: 001710303002

Examination Roll No: M4BPE19003

Registration Roll No: 140622 of 2017-2018

Under the Guidance of

DR. SUDESHNA SAHA

MASTER OF ENGINEERING IN BIOPROCESS ENGINEERING

DEPARTMENT OF CHEMICAL ENGINEERING

JADAVPUR UNIVERSITY

Jadavpur, Kolkata-700032

May 2019

Declaration of Originality and Compliance of Academic Ethics

I hereby declare that this thesis contains literature survey and original research work by the undersigned candidate, as part of her "***Master of Engineering in Bioprocess Engineering***" studies. All information in this document have been obtained and presented in accordance with academic rules and ethical conduct.

I also declare that, as required by these rules and conduct, I have fully cited and referenced all material and results that are not original to research *w*ork.

Name: **DEBALINA MONDAL**

Examination Roll Number: **M4BPE19003**

Thesis Title: **Chemical Synthesis of CNC Nanoparticles from Lignocelluloses and Their Application in Waste Water Treatment.**

Signature:

Date:

CERTIFICATION

To whom it may concern

This is to certify that **Debalina Mondal**, final year student of Master of Engineering in Bioprocess Engineering (M.BPE) examination student of Department of Chemical Engineering, Jadavpur University (Exam Roll No: M4BPE19003 ; Registration No: 140622 of 2017-2018), has completed the Project work titled **"Chemical Synthesis of CNC Nanoparticles from Lignocelluloses and Their Application in Waste Water Treatment"** under the guidance of **Dr. Sudeshna Saha** in the stipulated time during her Post Graduation Curriculum. This work has not been reported earlier anywhere and can be approved for submission in partial fulfilment of the course work.

Dr. Sudeshna Saha
Assistant Professor
Chemical Engineering Department
Jadavpur University, Kolkata-32

Prof. Debashis Roy
Head of the Department
Chemical Engineering Department
Jadavpur University, Kolkata-32

Prof. Chiranjib Bhattacharjee
Dean, Faculty of Engineering & Technology
Jadavpur University

ACKNOWLEDGEMENT

Though the following project is an individual work, I could never have reached the heights or explored the depths without the help, support, guidance and efforts of a lot of people. Firstly, I would like to thank my Project Guide, Dr. Sudeshna Saha (Assistant Prof Chemical Engineering) for instilling in me the qualities of being a good researcher. Her infectious enthusiasm and unlimited zeal have been major driving forces through my post graduate career at the Jadavpur University, Kolkata. This work would not have been possible without her.

I would also like to thank my laboratory co-researcher Gourab Ghosh and Sankhadeep Basu for their support during the project work. I would like to take this opportunity to thank Ms. Sujata Sardar, for her constant encouragement and helpful advice.

My very special thanks to my parents whom I owe everything I am today, my father Bansari Mohan Mondal and my mother Jhumur Mondal. Their unwavering faith and confidence in my abilities and in me is what has shaped me to be the person I am today. Thank you for everything.

Finally, I would like to take the opportunity to thank all my teachers and support staff of the Chemical Engineering Department, Jadavpur University, Kolkata.

ABSTRACT

Here nanocelluloses (CNC-I and CNC-II) are prepared by sulfuric acid hydrolysis of the pre-treatment residues obtained from Crotalaria Juncea. Prepared CNCs are characterized by FTIR, Powder XRD, SEM and BET studies. The different stretching vibrational peaks in FTIR spectra, suggesting presence of different functional groups in CNCs. In FTIR spectra, stretching frequency due to different functional groups of CNC-I is different from CNC-II indicating CNC-I and CNC-II are structurally not identical. XRD pattern of CNCs exhibit a number of crystalline peaks, but packing pattern of CNC-I and CNC-II are different. A number of micro-tubes of CNC are consist of nanotubes connecting side by side in parallelly manner are visualised from SEM images. The adsorption isotherms of the CNCs materials demonstrated steep nitrogen uptakes in the lower pressure region, suggesting their mesoporous nature. The Brunauer–Emmett–Teller (BET) surface area of CNC-I is 7.5 m^2 g^{-1}. The mesoporosity of the materials is probably due to the presence of interparticle voids or cages in the networks. The adsorption of methylene blue by CNC-I is significantly increased when varied the pH values from 5.0 to 10, suggesting at higher pH ionization of carboxyl acid groups and thus increase the interactions between negatively charged groups present in CNCs and dye cations. The adsorption of dye by CNCs is found to be better at the higher concentration of dye. The adsorption capacity of dye by CNCs is increased with increasing of activation times and it has been found that the highest capacity of adsorption is 58 % at 20 hours. From a comparison studies (dye adsorption) by taking five different CNCs materials using methylene blue and malachite green dye it has been found that, adsorption performance (adsorption of methylene blue) of a commercial bacterial CNCs is better than other. On the other hand, adsorption performance (adsorption of malachite green) of surface modified CNCs is better than normal CNCs. The stability of nanocellulose as adsorbent also shows good prospects in upgrading scale as regenerative aspects. This article provides a comprehensive analysis on the use of nanocellulose for the wastewater treatment.

Keywords: Crotalaria Juncea, Cellulose Nano Crystal, Adsorption, Waste Water Treatment

Contents

List of Figure

List of Table

CHAPTER-I

1.1 INTRODUCTION

In recent times most of the countries are facing drinking water problems and situations are severely critical in developing countries. Treatment of waste water to serve as drinking water over the global nation is a great challenge towards researchers. There are a number of techniques used for treatment of waste water i.e. chemical and physical prospects such as chlorine and it's derivatives, Ultraviolet light, boiling, low frequency ultrasonic irradiation, distillation, reverse osmosis, water sediment filters (fibre and ceramic), activated carbon, solid block, Pitcher and faucet-mount filters, bottled water, ion exchange water softener, ozonisation, activated alumina 'Altered' water etc. But research on nanotechnology mainly nanocellulose in waste water purification for safe drinking is a new way which need extensive research. Advantages on separation of various harmful bacteria, metal salts, metal ions, metals, dyes and organic contaminants, such as oils and cyclohexenes in waste water may be controlled by their variable Nano range pore size due to high surface density of various nanocelluloses. Cellulose nanocrystals (CNC) are generally rod-shaped nanoparticles, with lengths varying from 100 to 2000 nm, and diameters ranging from 2 and 20 nm while cellulose nanofibrils (CNF) are of several um in length (2-5) and diameters ranging from 20-100 nm, depending on the synthetic methods and nature of the cellulose (raw materials). There is no doubt that nanotechnology is better than any other technology, till now the environmental fate and toxicity of nanocellulose is still in infancy.

Wastewater contains both soluble compounds and small solid colloidal material ranging in particle size from 0.001 to 10μm. Colloidal particles increase the turbidity, colour and COD (chemical oxygen demand) of the water (Bratby 2006) and have a tendency to adsorb various ions from the surrounding medium which impart an electrostatic charge to the colloids relative to the bulk of the surrounding water in addition to dissociation (Wang *et al.* 2005, Bratby 2006). The small size of colloidal particles (<1μm) implies that sedimentation rates are very slow

compered to diffusion and thus a colloid remains stable as long as repulsive interactions between the particles prevent aggregation due to collisions (Wang *et al*. 2005). Thus colloids must be gathered together into larger aggregates in order to remove them and reduce the turbidity of municipal and industrial wastewater (Wang *et al.* 2005, Song *et al.* 2010). In coagulation, such aggregates can be produced using inorganic aluminium or iron-based metal salts or synthetic short chain polymers as coagulants. Alternatively, flocculation can be used to produce larger aggregates using high-molecular-weight polymers. In many cases combined coagulation-flocculation treatments are applied in order to achieve the most cost-effective treatment efficiency. Combined treatment can reduce the coagulant doses required, the volume of sludge and the ionic load of the wastewater (especially the level of aluminium), and thereby save in overall costs (Bolto & Gregory 2007) The chemicals typically used for flocculation are macromolecular, water soluble polymers such as synthetic polyacrylamides, polyacrylic acids and polystyrene sulphuric acids and their derivatives, which are not readily biodegradable (Chakrabarti *et al.* 2008, Brostow *et al.* 2009). Synthetic polymers are efficient for producing large-branched flocs (Singh *et al.* 2000), but these flocs typically have a low shear resistance and can easily be broken down, causing the release of organic compounds and an increase the quantity of fine particles in the purified water (Brostow *et al*. 2009, Zhou *et al*. 2014). Moreover, these polymers may also contain unpolymerized monomers and additives that can be neurotoxic and/or carcinogenic (Rudén 2004, Ho *et al*. 2010). In addition, synthetic polymers are typically produced from oil-based raw materials, which means that they are non-renewable. Consequently, there has been a growing interest in replacing oilbased flocculants with more sustainable natural bio-based alternatives, which also produce more shear-resistant flocs.

There has also been an expansion in industrial activities that produce wastewater containing many soluble compounds like, recalcitrance organic pollutants and heavy metals. Especially, the contamination of water with heavy metals is a serious cause of environmental and human health problems (Doan *et al*. 2008, Wan Ngah & Hanafiah 2008, Duan *et al.* 2013). Unlike organic waste, heavy metals are non-biodegradable and can accumulate in living tissues, causing various diseases and disorders, since they can be toxic and/or carcinogenic (Wan Ngah & Hanafiah 2008, Fu & Wang 2011). The heavy metals that are most commonly associated with pollution and toxicity problems include zinc (Zn), copper (Cu), nickel (Ni), mercury (Hg), cadmium (Cd), lead (Pb) and chromium (Cr) (O'Connell *et al.* 2008, Fu & Wang 2011).

Heavy metals can be removed from effluents using chemical reduction, electrochemical treatment, ion exchange, precipitation with hydroxides, carbonates and sulphides (Garg *et al*. 2008), evaporative recovery or adsorption onto activated carbon, for instance (Min *et al.* 2004, O'Connell *et al*. 2008, Gupta & Babu 2009). These methods are expensive and inefficient in many cases, however, especially when the metal concentration is low (<100 ppm) (Guzel *et al.* 2008, O'Connell *et al*. 2008, Gupta & Babu 2009). The sludge generated in the precipitation method also poses challenges in connection with its handling, treatment and disposal by landfilling, while ion exchange requires high capital and operational costs due to the chemicals used for the regeneration of resins (Doan *et al.* 2008, O'Connell *et al*. 2008). Electrolysis is an advantageous method if the concentration of metals is high, but it is inefficient at low metal concentrations (Doan *et al*. 2008, O'Connell *et al*. 2008) of all the treatments, adsorption is one of the most feasible and effective for removing heavy metals from wastewater. Activated carbon adsorbents are typically used for this purpose, but the high material costs are restrictive in many cases (O'Connell *et al*. 2008). Consequently, low-cost sorbents derived from abundant renewable resources, industrial by-products or waste materials have been considered as attractive alternatives for heavy metal removal (Babel & Kurniawan 2003, Crini 2005, Sud *et al.* 2008, Gupta & Babu 2009). Cellulosic waste materials such as sugarcane bagasse (Karnitz Jr *et al*. 2007), cotton linters (Nada *et al*. 2002) and wheat straw (Chojnacka 2006, Doan *et al.* 2008), have already been investigated for the adsorption Cd(II), Cu(II), Mn(II), Mg(II), Sr(II) and Pb(II) ions, for example, but more development work with regard to the adsorption performance and the regeneration of these bio sorbents is still needed for them to be viable options in commercial applications.

1.2 OBJECTIVES

The main objective of the project is to design and develop light weight nanocrystalline cellulose (CNC) aerogel as a super adsorbent for waste water treatment. The following are the specific objectives that need to be addressed at several steps of the present study:

- Pre-treatment- conversion of lignocellulose fibre to cellulose, to reduce the degree of polymerisation, moisture content, lignin content and to increase available surface area.
- Conversion of pre-treated pulp to nanocrystalline cellulose by acid hydrolysis

- Characterization of prepared CNCs for their size, shape, chemical structure, thermal properties etc.
- Process optimisation and intensification of CNC preparation from C. Juncea.
- Preparation of stable, lightweight, highly porous aerogel-membrane from the prepared CNCs and their characterizations using advanced analytical techniques.
- Evaluation of the efficacy of the prepared membranes for water treatment application.
- Study the effect of surface functionalization on the adsorption characteristic of the prepared membranes.

1.3 Novelty of the work

The novelty of this work lies in selection of natural resources, that the use of cellulose nanofibers (CNFs) as adsorbent for wastewater applications has been widely explored compared to the cellulose nanocrytals (CNCs). Although a number of literatures in the last couple of years have been devoted to explore the possibility to use CNCs as adsorbent for water treatment[1]–[4] , none has focused on the mechanism of adsorption and possible enhancement by surface functionalization as well as scale up opportunities. In addition, none of the report suggested development of membranes from CNCs which can further be used for water treatment applications. In this study a detailed procedure for extraction of CNCs from C. juncea fiber followed by membrane preparation using CNCs will be explored and presented along with the possible adsorption mechanism.

CHAPTER-II

2 Literature Review

In the last decade, research on nanocelluloses has skyrocketed due to their unique properties such as renewable, light weight, high aspect ratio and surface tuning abilities which make them viable for a specific application. In this report a brief overview about the nanocelluloses in waste-water application has been summarized.

Since inception of civilization cellulose has been used in the form of wood and plant fibres as an energy source, for building materials, paper, textiles and clothing. The use of cellulose based materials which is abundantly available in nature continues today in various industries.[5], and a substantial amount of cellulose found its uses in polymeric reinforcements in form of polymeric materials[6]. Cellulose plays an important role like reinforce element in the cell wall, generally together with lignin and hemicelluloses. These three polymers are closely associated making up lingo-cellulosic biomass. Actually, the lingo-cellulosic structure can be regarded as a bio-nanocomposite, which results from a unique interplay between Nano-scale domains of cellulose, hemicelluloses and lignin[7]. Nanocellulose being the eternal part of Cellulosic component has tremendous applications as nanocomposites [8]. Nano-Cellulose (also known as Crystalline Nano-cellulose, Nano-Crystalline Cellulose, Cellulose-Nano Whiskers)[9]. Nano-Cellulose can be isolated from nature including plants, animals (tunicates), bacteria and algae and in principle could be extracted from almost any cellulosic material some common examples are stated in Table 1**.** It employs different type of pre-treatment for removal of lignin and Hemicellulose and Hydrolysis with acid to remove the amorphous portion of cellulose.

The isolation of Nano-Cellulose from cellulose source materials occurs in two stages, i) Pre-treatment ii) Acid Hydrolysis.[10] For wood and plant source materials, the pre-treatments are similar and consist of techniques that are usually used in pulp and paper industry. In practice, lignin prevents separation of wood into its component fibers, so delignification is a necessary preparation step to produce Crystalline Nano-Cellulose(CNC).[11], [12]

2.1 Pretreatment of cellulose

2.1.1 Pulping and Bleaching Processes

Chemical treatment (pulping) of biomass previously chipped to depolymerize and eventually solubilize lignin and hemicelluloses, and a subsequent bleaching with oxidizing agents such as oxygen or $NaClO_2$. [13]

2.1.2 Stream Explosion Process

Method for converting lingo-cellulosic biomass with the final aim of separating nanofibers it applied specially to those biomass which can be hydrolyzed enzymatically. [14]

2.1.3 Acid hydrolysis extensively process

During acid hydrolysis amorphous domains are preferentially hydrolyzed, whereas crystalline regions have higher resistance to acid attack [15]. Acid hydrolysis extensively follows the following steps - [10]

1) Strong acid hydrolysis of pure cellulosic material under strictly controlled conditions of temperature, time, agitation, and with control of other conditions such as nature and concentration of the acid and the acid to cellulose ratio.

2) Dilution with water to stop reaction and repeated washing with successive centrifugation.

3) Extensive dialysis against distilled water to fully remove free acid molecules.

4) Mechanical treatment, usually sonication, to disperse then nanocrystals as a uniform stable suspension.

5) Freeze drying to yield dry CNC/NCC.

However, sulphuric acid is mostly used for acid treatment.[16]

Ever increasing global demand of sustainable development of eco-friendly products by using natural resources, has catalysed the way for various research works on biomaterials such as cellulose and thus the potential of micro and nano sized celluloses for high end applications has been explored in recent years. [17]Nanocelluloses are highly prospective material for water treatment they possess the fundamental cellulose characteristics such as hydrophilicity, wide fictionalization ability, and the ease of fabrication of variable semi crystalline fiber textures with the nanoscale properties like large surface area, high aspect ratio, quantum size effects as well as chemical accessibility [18]. Nanocelluloses are bio degradable materials which offer attractive

properties like flexibility, toughness, low density and high adsorption capacity. They are also biocompatible, biodegradable and environmental friendly.

Nano-cellulose based adsorbents can be classified as:

a) Carboxylated cellulose nanomaterials[19]

b) Succinylated nanocelluloses [20]

c) Amino–modified nanocelluloses [21]

Cellulose Nanocrystals has been clubbed with many materials to form nano-composites for the adsorption of heavy metals from waste water. Some popular nano-cellulose used as adsorbents are stated under:

i) Magnetic cellulose nanocomposites [22][23]

ii) Cellulose/Silsesquioxane nanocomposite [24], [25]

iii) Cellulose/Clay nanocomposite [26]

iv) Cellulose/Polymer nano-composites [26][19]

CNCs have wide application as reinforcing agent and as adsorbent [22], in Table 2.2 the uses of nanocelluloses as the adsorbent from the waste water is studied and the capacity of adsorption are stated also.

2.2 Adsorption

Adsorption is known to be an effective and economic method for removing impurities from wastewater. Adsorption can be a reversible process, which implies possible regeneration of the adsorbents through suitable desorption processes (Fu & Wang 2011). Adsorption of a molecule or ion from a solution to the surface of an adsorbent involves three steps: 1) removal of the molecule from the solution, 2) removal of the solvent from the solid surface, and 3) attachment of the molecule to the surface of the solid (Crini 2005, Bratby 2006). Either a hard or a soft classification can be used to predict how different functional groups will bind particular metal cations. According to these classifications, acids and bases have an attractive interaction and the most stable interactions are hard acid-hard base and soft acid-soft base ones. Hard acids preferentially bind to ligands containing oxygen, while soft acids preferentially bind to ones containing S and N (Gadd 2009, Hubbe *et al*. 2011). The hard/soft scheme predicts that bonds formed between hard acids and hard ligands will be predominantly ionic, whereas soft acid-ligand complexes are more covalent in character (Gadd 2009). These definitions are not absolute,

and variations may cause by metal concentrations, for example, or by the relative metal concentrations in mixtures where competitive effects may occur (Gadd 2009).

Adsorption mechanisms are dependent on the degree of adsorbate-adsorbent interaction and the adsorbate-solvent interactions (Ho *et al.* 2000). Adsorption processes may include physical and chemical adsorption like, ion exchange and chemical complexation (Ho *et al*. 2000, O'Connell *et al*. 2008). It is also possible for more than one of these mechanisms to be present and affect the adsorption interaction (Crini 2005, O'Connell *et al*. 2008, Gadd 2009). In the case of the uptake of metals by bio-based sorbents, ion exchange and chemical complexation are the most common mechanisms (Doan *et al*. 2008, Gupta *et al*. 2009).

2.2.1 Ion exchanging for the adsorption process

Ion exchange is the mechanism by which adsorbing metal ions take the place of other species already associated with the sorbent surface. Thus it is the replacement of an adsorbed, readily exchangeable ion by another (Gadd 2009). These entities may be ions such as Na^{+}, Ca^{2+} or proton H^{+} (Dą browski *et al*. 2004, Hubbe *et al*. 2011). Higher affinity for exchanged ion will lead to desorption of an associated ion from surface sites and uptake of an exchanged ion (Hubbe *et al*. 2011). Ion exchange is mainly concerned with the stoichiometry of the displacement of bound ions by dissolved ions (Hubbe *et al.* 2011). In chemical complexation, the functional groups of the adsorbent surface have site-specific interactions with particular kinds of metal ions (Sud *et al*. 2008, Hubbe *et al*. 2011) (Fig. 2.1). A molecule or ion can be held on the solid surface by ionic, covalent, hydrogen or dipolar bonding, i.e. processes of chemical adsorption (Bratby

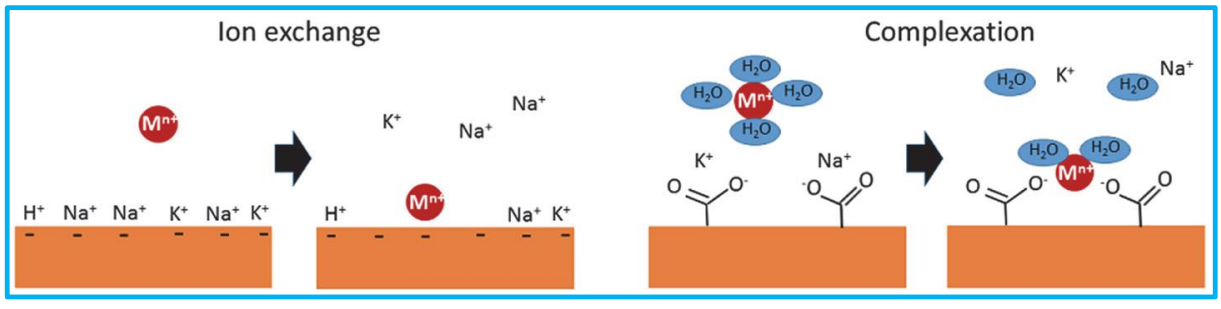

Figure 2.1 Illustration of the ion exchange (left) and chemical complexation (right)

2006), while adsorption processes arising from van der Waals attraction are referred to as physical adsorption (Bratby 2006). In chemical complexation the ability of a surface site to bind various metals is attributed to the radius of the metal ion and the symmetry of its valence electron orbitals relative to the positions of the surface-bound atoms at the site of adsorption (Hubbe *et al*. 2011).

2.2.2 Removal of metal ion by adsorption process

The removal of metal ions from aqueous solutions by adsorption depends on the solution's pH, the degree of ionization of the different species and the surface characteristics of the adsorbent (Karnitz Jr *et al*. 2009). Thus the pH can influence the protonation of the functional groups on the adsorbent as well as the solution chemistry of the metal ions (Liu *et al*. 2010). Predicting the rate at which adsorption takes place for a given system is an important part of adsorption system design (Sud *et al*. 2008). Numerous kinetic models are available, such as first-order and second-order reversible ones and firstorder and second-order irreversible ones, and also pseudo-first-order and pseudosecond- order ones, to describe the reaction order of adsorption systems based on the concentration of the solution (Sud *et al*. 2008, Gadd 2009, Hubbe *et al*. 2011). The adsorption process is often characterized using a number of isotherm models. These isotherms represent the relationship between the amount adsorbed per unit weight of solid sorbent and the amount of solute remaining in the solution at equilibrium (Sud *et al*. 2008). These include the most common Langmuir (1918) and Freundlich (1926) isotherms and other related models (Altin *et al*. 1998, O'Connell *et al.* 2008, Hubbe *et al.* 2011). The Langmuir and Freundlich models are widely used, since they are simple and are able to describe the experimental results over a wide range of concentrations (Altin *et al*. 1998, Perić *et al*. 2004). They have also been found to fit best with most of the biosorbents, including cellulosic adsorbents (O'Connell *et al*. 2008, Hubbe *et al*. 2011, Hubbe *et al*. 2012). Mathematical correlation of the Langmuir isotherm has provided a basis for developing other models, which include the similarity between adsorption and ion exchange, Gaussian energy distribution, degree of surface heterogeneity and the range of high solute concentrations (Perić *et al*. 2004, O'Connell *et al*. 2008). The most commonly used Langmuir isotherm defines the equilibrium parameters of homogenous surfaces, monolayer adsorption and the distribution of adsorption sites (Perić *et al*. 2004, O'Connell *et al*. 2008, Hubbe *et al*. 2011).

2.3 Wastewater treatment

There are number of treatment processes available for the removal of solids and soluble impurities from wastewater. These can be categorized into physical, chemical or biological treatments, and include processes such as sedimentation, precipitation, extraction, evaporation, coagulation-flocculation, flotation, electrocoagulation, filtration, adsorption, ion exchange, bio-degradation and electrochemical treatment (Harif *et al*. 2012, Das *et al.* 2013, Sher *et al*. 2013). The efficient treatment of wastewater usually requires a number of steps, and it is often appropriate to combine more than one method (Sher *et al.* 2013). Coagulation and flocculation are amongst the most widely practised technologies for removing solids from industrial and municipal wastewater, while adsorption is the method most frequently used metals in dilute solutions (Gadd 2009, Fu & Wang 2011).

2.3.1 Natural polymers in wastewater treatment

In view of the increased demand for "green" and sustainable water treatment technologies, natural polymers have been widely investigated as means of replacing synthetic and inorganic water chemicals (Song *et al*. 2010). Biodegradability is one of the most important environmental aspects of water chemicals, as it will affect their long-term ecological impact (Xing *et al*. 2010). On the other hand, biochemicals derived from cheap, unwanted by-product possessing high performance, e.g. high selective adsorption capacity, are to be preferred (Wan Ngah & Hanafiah 2008, Dang *et al*. 2009). In recent years it has been polysaccharides such as guar gum (Banerjee *et al*. 2013), starch (Abdel-Aal *et al*. 2006, Xing *et al*. 2010), chitosan (Lu *et al*. 2011, Yang *et al*. 2011), cellulose (Song *et al*. 2010) and their derivates such as dextran (Ghimici *et al.* 2009, Ghimici & Nichifor 2010 and pullulan (Ghimici *et al*. 2010, Constantin *et al*. 2013) that have particularly attracted attention as flocculation and adsorption aids (Zhang *et al*. 2013).

2.3.2 Types of cellulose

Cellulose is the most abundant renewable biopolymer on the Earth (Saito & Isogai 2005). Natural cellulose fibres are prevalent throughout the world in plants such as grasses and reeds and in the stalks and woody parts of the vegetation in general (Azizi Samir *et al*. 2005). The worldwide production of cellulose is estimated to be between 1010-1011 tons each year (Azizi

Samir *et al*. 2005, Habibi *et al*. 2010, Lavoine *et al*. 2012, Abdul Khalil *et al*. 2014), and with only about 6 × 109 tons of this processed the paper, corrugating, chemical and textile industries (Simon *et al*. 1998, Lavoine *et al*. 2012). In general, cellulose is a strong, fibrous, water-insoluble substance that plays an essential role in maintaining the structure of plant cell walls (Habibi *et al*. 2010). The properties of cellulosic fibres are greatly influenced by factors such as their chemical composition, internal fibre structure, microfibril angle, cell dimensions and defects, which vary between plant species and between parts of the same plant (Siqueira *et al*. 2010). Regardless of its source, cellulose can be characterized as a high-molecular-weight linear homopolysaccharide of β-1,4-linked anhydro-Dglucose units in which every unit is corkscrewed 180° with respect to its neighbours (Habibi *et al*. 2010, Siqueira *et al*. 2010). The repeating segment is frequently taken to be a dimer of glucose known as cellobiose (Habibi *et al*. 2010, Siqueira *et al*. 2010), while the monomer, named the anhydroglucose unit (AGU), bears three hydroxyl groups, which confer upon cellulose its most important properties, its multi scale micro fibrillated structure, its hierarchical organization, of crystalline versus amorphous regions and its highly cohesive character (Lavoine *et al*. 2012). In nature, cellulose chains have a DP of approximately 10 000 anhydro glucopyranose units in wood and 15 000 units in cotton (Azizi Samir *et al*. 2005, Siqueira *et al*. 2010).

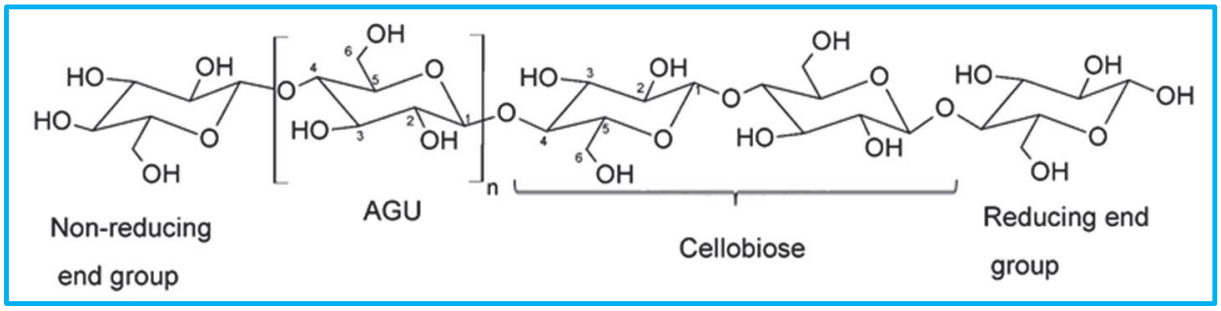

Figure 2.2 Structure of cellulose with carbon atoms numbered in AGU and showing the repeating cellobiose unit in cellulose.

(i) Nanocelluloses

Nanocelluloses, elemental nano-sized constituents of plant fibres, have acquired an extra reputation relative to conventional cellulose fibres due to their huge surface area, high aspect ratio and high Young's modulus of 145 GPa (Iwamoto *et al*. 2009) resulting from high crystallinity (Klemm *et al*. 2011, Abdul Khalil *et al*. 2014, Jin *et al*. 2014). Furthermore, being as nature materials, nanocelluloses are biodegradable, biocompatible and renewable (Jin *et al*.

2014). The lateral size of cellulose molecule chains is about 0.3 nm, and these chains form bundles of elongated fibrils still with nano-scale diameters. The cellulose chains are stabilized laterally by hydrogen bonds between their hydroxyl groups (Zimmermann *et al*. 2004).

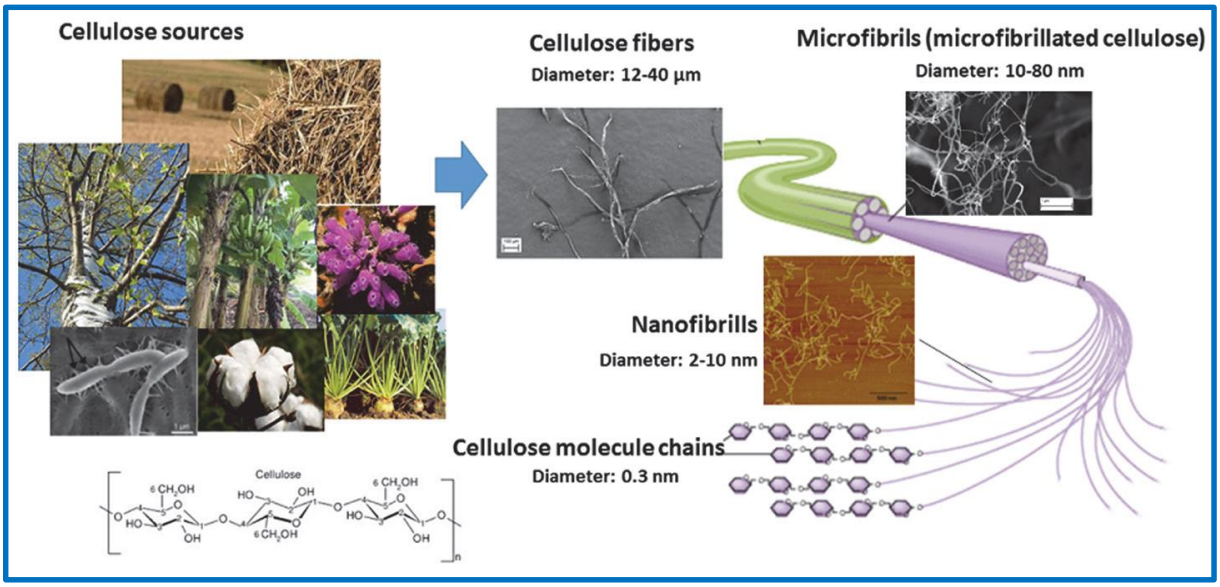

Figure 2.3 From the cellulose source to the cellulose molecules

There are three main categories of nanocelluloses (Klemm *et al*. 2011); nanofibrillated celluloses, nanocrystalline celluloses and bacterial celluloses. Nanofibrillated celluloses are elongated strains of superfine fibrils, while nanocrystalline celluloses are rod-like particulates consisting of crystalline cellulose (Zimmermann *et al*. 2004, Siqueira *et al*. 2010, Abdul Khalil *et al*. 2014). Bacterial cellulose is produced by down-to-top synthesis, where specific bacteria synthetize bundles of cellulose nanofibrils from low molecular sugars and alcohols (Klemm *et al*. 2011). The focus in this thesis will be on the nanofibrillated celluloses.

Nanocelluloses can be produced from cellulose pulp using pure mechanical or combined chemical or enzymatic and mechanical treatments. The chemical and enzymatic pre-treatments reduce the energy needed for individualization of the nanofibrils. These treatments typically reduce the hydrogen bonds and/or add a repulsive charge, or else reduce the DP or the amorphous part between the individual nanofibrils (Lavoine *et al*. 2012).

(ii) Nanofibrillated Celluloses

Nanofibrillated celluloses exhibit both amorphous and crystalline parts (60%-80%) in their flexible fibrillar strands, which have typical lateral dimensions of 2-80 nm and are several micrometres in length (Klemm *et al.* 2011, Lavoine *et al.* 2012, Abdul Khalil *et al*. 2014). They also have a very high surface area, in the range 170-246 m^2g^{-1}, (as measured from a nanocellulose and polypyrrole aerogel composite (Carlsson *et al*. 2012).

2.4 Chemical and Structural Composition of Cellulose Fibers

Cellulose is a high molecular weight natural homopolymer, composed of α-1,4-linked anhydro-D-glucose units. The sugar units are linked by combining the H and –OH group together with the elimination of water. Linking two of these sugars produces a disaccharide called cellobiose. The glucose units are in 6-membered rings, called pyranoses. They are joined by single oxygen atoms (acetal linkages) between the C-1 of one pyranose ring and the C-4 of the next ring. Since the water molecule is lost due to the reaction of an alcohol and a hemiacetal to form an acetal, the glucose units in the cellulose polymer are referred to as anhydroglucose units. The cellulose molecule contains three different kinds of anhydroglucose units, the reducing end with a free hemiacetal (or aldehyde) group at C-1, the nonreducing end with a free hydroxyl at C-4 and the internal rings joined at C-1 and C-4 (Figure 2.4).

The stereochemistry at carbons 2, 3, 4 and 5 of the glucose molecules are fixed, but in pyranose form, the hydroxyl at C-4 can approach the carbonyl at C-1 from either side, resulting in two different stereo chemistries. If the hydroxyl group at C-1 is on the same side of the ring as the C-6 carbon, it is said to be in the α configuration. In cellulose, the C-1 is positioned oppositely producing β configuration. Functional groups of cellulose β configuration are in equatorial positions, making the cellulose molecular chain to be more or less extended in straight line.

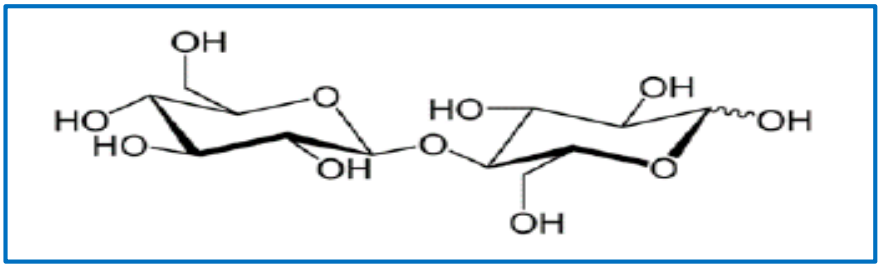

Figure 2.4 Cellobiose unit

In nature, cellulose does not occur as an isolated individual molecule. Although cellulose is biologically synthesized as individual molecules, they undergo spinning in a hierarchical order at the site of biosynthesis. In the case of primary cell wall of plants, glucose residues are polymerized into cellobiose unit (redrawn from). In nature, cellulose does not occur as an isolated individual molecule. Although cellulose is biologically synthesized as individual molecules, they undergo spinning in a hierarchical order at the site of biosynthesis. In the case of primary cell wall of plants, glucose residues are polymerized into individual chains. Later, 36 chains are assembled together to form a microfibril. During synthesis of the plant secondary wall, microfibrils often associate further to form bundles (Figure 2.5). However, the chain length may varies ranging from as low as 2000 up to 20,000 glucose residues.

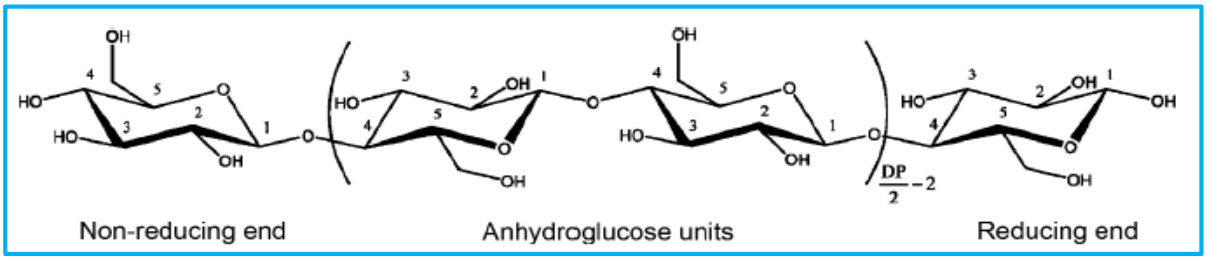

Figure 2.5 Chemical structure of cellulose

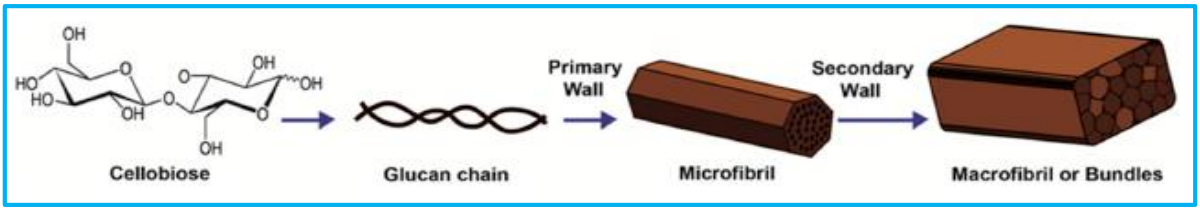

Figure 2.6 Glucose residues polymerized into individual chain and further assemble into microfibrils and microfibrils or bundles.

In the ordered regions, cellulose chains are tightly packed together in crystallites, which are stabilized by a strong and very complex intra and intermolecular hydrogen-bond network. The hydrogen bonding network and molecular orientation in cellulose can vary widely, which can give rise to cellulose polymorphs or allomorphs. Six interconvertible polymorphs of cellulose, namely, I, II, IIII, IIIII, IVI, and IVII, have been identified. Meanwhile the amorphous regions are distributed as chain dislocations on segments along the elementary fibril where the microfibrils are distorted by internal strain in the fiber and proceed to tilt and twist. Native cellulose has been thought to have cellulose I shape.

2.5 Modification of CNCs using TEMPO

One of the most widely used chemical pretreatment is TEMPO (2,2,6,6 tetramethyl-1-piperidinyloxy)-mediated oxidation, which selectively converts the C_6 primary hydroxyl groups of the cellulose to carboxylate groups via aldehyde groups under alkaline aqueous conditions using catalytic amounts of TEMPO (Saito & Isogai 2005, Isogai *et al*. 2011, Lavoine *et al*. 2012). As a result, the cellulose fibre structure can easily be disintegrated to individual nanofibrils due to repulsive forces among the ionized carboxylates (Lavoine *et al*. 2012). Another potential chemical oxidation pretreatment reaction for the production of nanocelluloses is periodate oxidation. In this reaction the C2 and C3 bonds of cellulose are selectively cleaved, yielding 2,3-dialdehyde cellulose, which can be further derivatized with functional groups such as carboxylic acids (Kim & Kuga 2001; Liimatainen *et al.* 2012b), sulphonic groups (Rajalaxmi *et al*. 2010, Liimatainen *et al*. 2012a, Liimatainen *et al.* 2013b) or imines (Sirviö *et al*. 2011a). Only a few previous studies of the use of nanocelluloses as water chemicals exist and they mainly address adsorption applications. TEMPO-oxidized nanocelluloses have been used for the adsorption of various metals from aqueous solutions, most efficiently with lead, calcium and silver (Saito & Isogai 2005). Succinic anhydride-modified mercerized nanocellulose (Hokkanen *et al*. 2013) and amino-modified nanocelluloses (Hokkanen *et al*. 2014) showed high efficiency in the removal of metal ions, with good regeneration ability, while Kardam *et al*. (2014) achieved improved heavy metal adsorption capacity subjecting rice straw cellulosics to acid hydrolysis, which produced rod-like cellulose nanocrystals. Yu *et al*. (2013) used carboxylated cellulose nanocrystals for the adsorption of heavy metals with good results, as adsorption was fast, with high capacity, and the adsorbent was easy to regenerate. In flocculation applications, TEMPO-oxidized nanocelluloses with CPAM were used to flocculate kaolin clay suspensions, whereupon relative turbidity decreased greatly and the resulting flocs were stronger than with CPAM alone (Jin *et al*. 2014).

Table 2.1 Size and shape CNCs from various sources

Source	L, nm	d, nm	References
Bacterial	100-1000	10-50	[27]
Tunicate	1160	16	[28]
Valonia	>1000	10-20	[29]
MCC	500	10	[30]
Cotton	255 100-150	15 5-10	[31] [27]
Cotton Linter	25-320 300-500	6-70 15	[32] [33]
Softwood	100-150	4-5	[34]
Hardwood	140-150	4-5	[34]
Wheat Straw	150-300	5	[35]
Rice straw	117	8-14	[36]
Coconut husk fiber	200	5.6	[37]
Waste Paper	100-300	3-10	[38]
Ramie	100-200	3-10	[39]
Sisal	100-500	3-5	[40] [41]
Carded and pristine hemp	100-200	15	[42]
Waste Sugar cane Bagasse	70-90	18-32	[10]
Marginata(Agave angustifolia)	240-390	8	[43]

Table 2.2 Application of CNCs on waste water treatment and heavy metal removal

Cellulose nanoparticles used as composites	Metal Adsorbed	Capacity of Adsorbent	References
Mechanochemical maghemite	As(V)	10-5015.0 mg g^{-1}	[44]
Succinic anhydride–modified mercerized nanocellulose	Zn(II)	1.610 mmol g^{-1}	[45]
Fe2O3 nanomaterial	As(III)	1.3 mg g^{-1}	[46]
Bacterial cellulose nanocomposite	Pb(II)	65.0 mg g^{-1}	[47]
Cellulose nanocrystals	Pb(II)	367.6 mg g^{-1}	(Yu, Tong, Ge, Wu et al., 2013)
Nano magnetic cellulose	Cu(II)	1.5 mmol g^{-1}	[22]
Fe2O3 nanomaterial	As(V)	4.6 mg g^{-1}	[46]
Carbonated hydroxyapatite modified nanocellulose	Ni(II)	2.021 mmol g^{-1}	[17]
Carbonated hydroxyapatite modified nanocellulose	Cd(II)	1.224 mmol g^{-1}	[17]
Carbonated hydroxyapatite modified nanocellulose	PO^{3-}_4	0.843 mmol g^{-1}	[17]
Carbonated hydroxyapatite modified nanocellulose	NO_3	0.209 mmol g^{-1}	[17]
Aminopropyltriethoxysilane (APS) modified nanocellulose	Ni(II)	2.734 mmol g^{-1}	[17]
Aminopropyltriethoxysilane modified nanocellulose	Cu(II)	3.150 mmol g^{-1}	[17]
Aminopropyltriethoxysilane modified nanocellulose	Cd(II)	4.195 mmol g^{-1}	[17]

2.6 Cellulose and its hierarchical structures

Cellulose is a polysaccharide consisting of a linear chain of several hundreds to over ten thousand β-(1-4)-linked D-glucose units with the formula $(C_6H_{10}O_5)$ n (Updegraff, 1962). Cellulose is a tasteless, odorless and hydrophilic material with a contact angle of 20-30° and cannot be dissolved in water or most organic solvents (Kamm et al., 2008). It is mainly isolated from wood and plant cell walls but can also be obtained from other biomass sources, such as carrots (Jonoobi et al., 2014) and potato peels (Chen et al., 2012). Cellulose is also synthesized by bacteria (Gluconacetobacter xylinus), algae (Valonia) and even animals (tunicates) (Osullivan, 1997). As a carbohydrate polymer, cellulose has a large number of hydroxyl groups that are capable of forming intra and inter-molecular hydrogen bonds. In nature, cellulose does not occur as an isolated individual molecule. Instead, cellulose comprises self-assembled individual cellulose chains forming fibers. Cellulose has a hierarchical structure, building up from the nano-scale to the microscale. Typically, approximately 36 glucan chains are assembled together through various bonds (van der Waals and hydrogen bonds) into elementary fibrils with 3-nm diameters, which pack into larger units called microfibrils. In turn, microfibrils are assembled into the familiar cellulose fiber.

2.7 Why nanocellulose-based membranes for water purification

The hydroxyl groups of cellulose protrude laterally at the equatorial positions along the cellulose chain and are readily available for hydrogen bonding. These hydrogen bonds cause chains to group together in highly ordered structures, thus making them mechanically stable. Good mechanical strength and rigidity can offer resistance to high-pressure environments in real water purification applications. Nanocelluloses have highly crystalline lattice structures that provide the chemical stability required to work within different pH ranges. Oksman et al. (2011) reported the crystallinity of nanocelluloses in the range of 70-80% depending on the process of isolation. Furthermore, the high crystallinity value makes nanocellulose resistant to acid washes during membrane regeneration and recovery of valuable filtrates. Membrane stability in water environment and hydrophilicity are advantageous for water treatment. Hydrophilicity reduces bio-fouling and organic fouling. However, due to the hydrophilic nature of nanocellulose, their utilization in membrane applications involving hydrophobic media is limited and restricts their

exploitation in non-aqueous media. The high surface area of nanocellulose provides a large number of active sites for interaction with and immobilization of pollutants. Recently, Sehaqui et al. (2011) reported a surface area of 482 m^2/g for a sheet comprising cellulose nanofibers prepared using supercritical CO_2 drying. However, the maintenance of this high surface area would be challenging during membrane processing. The presence of large numbers of functionalities within nanocellulose enables their use as a unique platform for significant surface modification through various chemistries (Habibi, 2014). The introduced functional groups can be tailored for the binding of specific or desirable pollutants from water. Volesky (2007) tested various functional groups, such as carbonyls (ketone), carboxyls, sulfhydryls (thiol), sulfonates, thioethers, amines, secondary amines, phosphates, phosphodiesters and imidazoles for various bio-residues. Our group has shown that the surface presence of COO^-, SO_3^-, and PO_3^{2-} makes nanocellulose selective toward positively charged species (Liu, 2014).

CHAPTER-III

3. Experimental Methods

3.1 Experimental Design

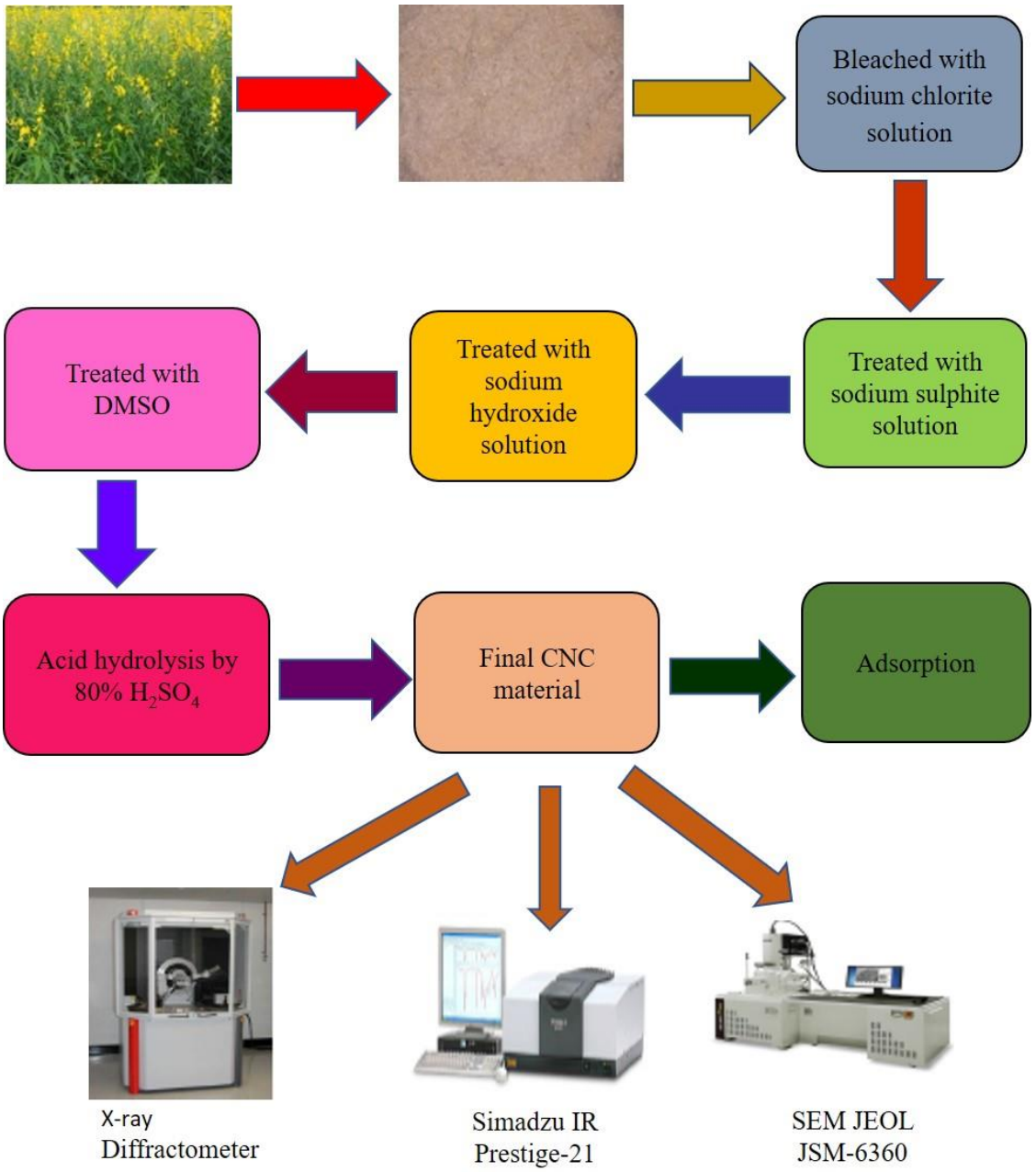

Figure 3.1 Schematic of overall experimental plan

3.2. Raw Material for CNC

3.2.1 Raw Material

The Crotalaria juncea fibers were cut to1-2cm in size using iron scissors. The particle size of the raw material was further reduced by using Wiley mill equipped with a 200 mesh.

3.2.2 Chemicals used

- Sodium Chlorite Solution (0.7% w/v) (Merck)
- Acetic Acid Solution (Merck)
- Sodium Sulphite Solution (5% w/v) (Merck)
- Sodium Hydroxide Solution (Merck)
- Dimethyl Sulfoxide (Merck)
- Sulphuric Acid Solution (Merck)
- Bacterial CNC (Himedia)
- PEG (Sigma Aldrich)
- TEMPO (Sigma Aldrich)
- Methylene Blue (E. Merck)
- Distilled Water

3.3 Preparation of CNC

Preparation of cellulose nanocrystals (CNCs) from lignocellulosic biomass mainly consist of two steps e.g., a) Pre-treatment and b) Hydrolysis. In the present study two different pre-treatment methods (namely pre-treatment-I and pre-treatment-II) were explored to evaluate their efficacy and compared.

3.3.1 Pre-treatment-I

Pre-treatment-I consisted of four steps as elaborated by Mandal and Chakrabarty[10]. In a typical experiment, 1 gm of the as prepared fiber was treated with 50 ml of 0.7 % (w/v) sodium chlorite solution at its boiling temperature. The reaction was carried out for 5 hrs at pH 4, adjusted by 5% acetic acid and maintained with buffer solution of pH 4 throughput the experiment to remove the

lignin. The residue was subsequently washed with distilled water until neutralized and oven-dried at 40 °C for overnight (PM-1).

This neutral residue (PM-1) was then boiled with 250 ml of 5% (w/v) sodium sulphite solution for 5 hours. Then the residue was washed with adequate distilled water to remove the lignin completely and hemicellulose partially and dried (PM-2).

The holo-cellulose (PM-2) thus obtained was further treated with 250 ml of 17.5% (w/v) sodium hydroxide solution for 5 hours at the boiling condition to remove the hemicelluloses. At the end of the extraction, the insoluble residue (cellulose) was collected by filtration and washed thoroughly with distilled water until the filtrate was neutral. Then the resulting cellulosic materials were air-dried (PM-3). PM-3 was further treated with 50 ml dimethyl sulfoxide (DMSO) at 80 ˚C in an oil bath for 3 hours. This additional step was introduced to increase the porosity into the cellulose rich substrate. The product thus obtained was then filtered, washed with distilled water and air-dried (PM-4).

3.3.2 Pre-treatment-II

An alternate method was devised by us to pre-treat CJ to obtain CNC. In a typical experiment, 5 gm of the milled Crotalaria juncea fiber was dispersed in 300 ml of distilled water using ultra-sonication (35 KHz Bio base Sonicator bath) at 50^{o}C for about 30 min. After sonication the aqueous suspension was left for drying at hot air oven at 100^{o}C for about 3 hours and then left under vacuum for overnight. The dry residue was mixed with 200 ml 5wt% NaOH. To the suspension 11wt% H_2O_2 was added drop-wise for about 5 minutes under continuous sonication. The experiment was carried out for 2 hours at 50^{o}C. Then the residue was washed with distilled water and dried under hot air oven followed by overnight vacuum (PM-5).

3.3.3 Acid-Hydrolysis

After both the pre-treatments dried residues (PM-4 and PM-5) was subjected to acid hydrolysis by heating with 80 % (w/w) sulphuric acid (fiber to liquor ratio of 1:20) for 5 hours and 1 hours at 50˚C under strong agitation respectively yielding CNC-I and CNC-II. The hydrolysis was quenched by adding 5-fold excess water (100 ml) to the reaction mixture. The resulting mixture was cooled to room temperature and centrifuged. Then it is freeze dried (Labogene Coolsafe) to obtained powdered CNCs for further tests.

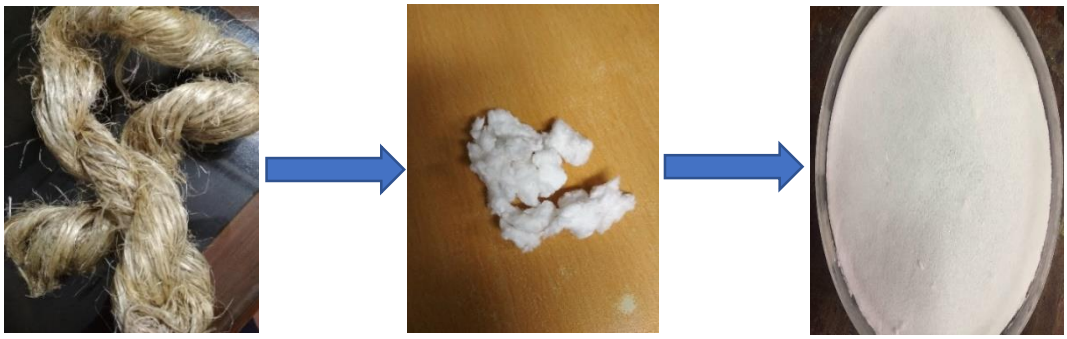

Figure 3.2 Conversion of raw material to CNC

3.4 Preparation of TEMPO oxidise CNC

Freeze dried CNC (1076 mg) was taken in 500 ml beaker and 100 ml deionised water was added to it and stir thoroughly. NaBr (322 mg) was added to it after that TEMPO (16.6 mg) was added to the stirrer solution of CNC. Then 13 % NaOCl 8.1 ml was added to the solution mixture dropwise over 25 minutes. Thereafter, NaOH solution (0.5 mol/lit) was added to the reaction mixture to make its pH 10, the reaction mixture was stirred continue for 1 hour.

Figure 3.3 Images of CNC Membrane

Then, methanol 4 ml was added to the mixture of solution. Thereafter, HCl (0.5 mol/lit) was added to the reaction mixture to adjust pH 7 of the solution. Then, the mixture of solution was centrifuged for five times and after that, it was kept in freeze dried for overnight. Finally, TEMPO CNC was collected as a white membrane.

Figure 3.4 Image of instruments (a) (b) Incubator shaker, (c) Hot plate stirrer and (d) Sonicator

3.5 Characterization of prepared CNC and surface modified CNC

Several techniques were employed for the characterization of the samples. The structural variations of CNC were examined by FTIR spectroscopy using a JASCO FT/IR -4700 spectrophotometer. The FTIR spectrum of the samples was noted in the transmittance mode in the range of 4000-450 cm^{-1}. The structural analysis of the sample was studied using an X-ray diffractometer (Ultima III Rigaku) with Cu kα radiation source operating at 40 kV and 30 mA. Scattered radiation was detected in the range of $2\theta = 10^0$-80^0, at a scanning rate of 2^0 min^{-1}. The surface morphology of the prepared cellulose was investigated using a scanning electron

microscopy (SEM) through ZEISS SEM instrument (Model: ZEISS EVO-MA10) operating at 15 kV after Platinum coating. Morphological images of the samples were taken at different manifestations. Nitrogen adsorption/desorption isotherms were conducted using a Quanta chrome Instruments Autosorb 1C BET surface area analyser. Before the analysis the samples were degassed at 193 K for 3 h under high vacuum. Spectroscopic analysis of the products was carried out using a Perkin Elmer model (Lambda) UV-vis spectrophotometer.

CHAPTER-IV

4. Result and Discussion

4.1 Characterizations of CNCs

The CNCs obtained using two different pre-treatment techniques were characterized further to evaluate the chemical structure (FTIR spectra) and crystalline nature (XRD). In addition, determination of degree of sulfation helped to calculate the attachment of surface half ester groups during acid hydrolysis.

4.1.1 Fourier Transform Infrared Spectroscopy (FTIR)

FTIR analysis of the prepared CNCs revealed chemical structure associated with these samples. The peak at 3411 cm^{-1} signifies the presence of –OH group, as the peak is bulgy. The most prominent band in alcohols is due to the O-H bond, and it appears as a strong, broad band covering the range of about 3000 - 3700 cm^{-1}. A carboxylic acid functional group combines the features of alcohols and ketones because it has both the O-H bond and the C=O bond. Therefore, carboxylic acids show a very strong and broad band covering a wide range between 2800 and 3500 cm^{-1} for the O-H stretch. At the same time they also show the stake-shaped band in the middle of the spectrum around 1710 cm^{-1} corresponding to the C=O stretch which was absent for both CNC-I and CNC-II [10]. Peak around 3000 cm^{-1} signifies C-H stretching vibrations originating from methyl group in this FTIR result. The peak around 2965 cm^{-1} can be attributed to the C-H stretching of methyl groups and/or aromatic ring vibrations. While the bands at 1178cm^{-1} and 1073 cm^{-1} were mainly due to anti-symmetric stretching vibrations of C-O-C bridge and also skeletal vibrations involving C-O stretching which contributes to the cellulose backbone respectively. These were assigned to be characteristics band of saccharide structure[48], [49]. The band at 906 $cm^{-1}$was the characteristic peak of glyosidic bonds which is present in the cellulose [50]. The other entire spectrum beyond 1500 to 500 cm^{-1} lies in the fingerprint region [51]. From the FTIR spectra (Figure 4.1) it has been observed that both are cellulose rich substrate and lignin was completely removed for both CNC-I and CNC-II. It was

also observed that CNC-I showed a much sharper characteristic peak of glycosidic bonds compared to that of CNC-II.

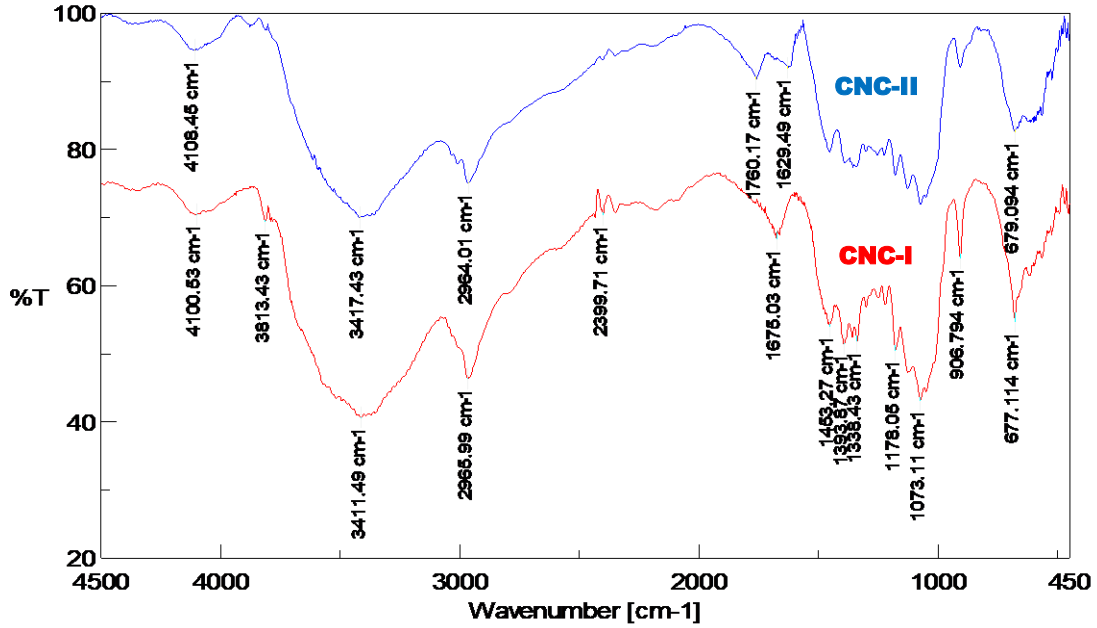

Figure 4.1 FTIR spectra of CNC-I and CNC-II

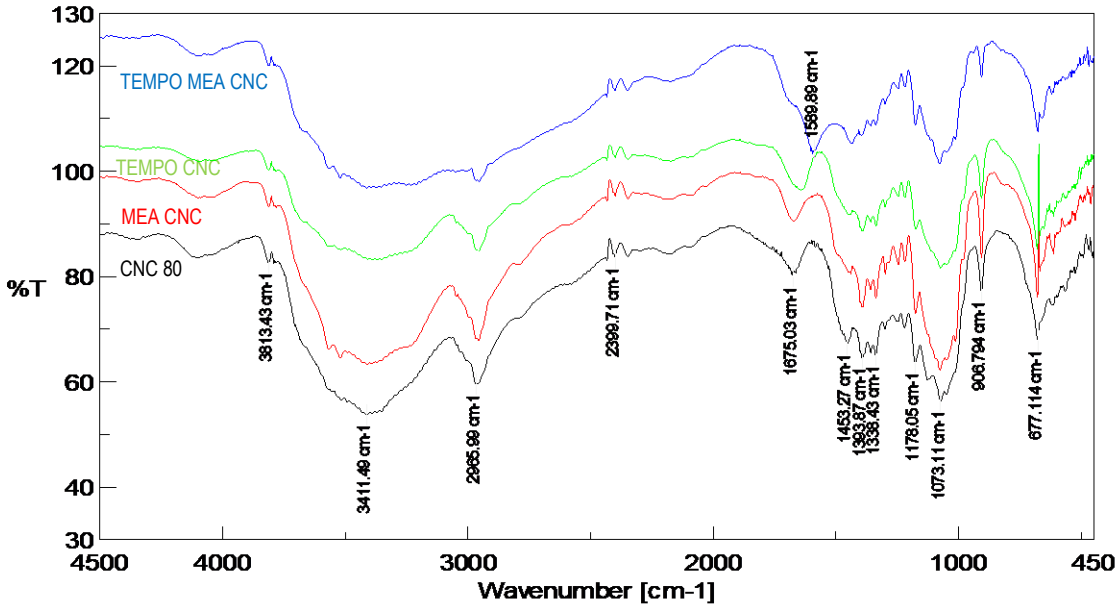

Figure 4.2 FTIR spectra of TEMPO MEA CNC, TEMPO CNC, MEA CNC, CNC

The FTIR studies of TEMPO-MEA-CNC, TEMPO-CNC, MEA-CNC and CNC-80 have been done, which are presented in figure 4.2. From the figure it has been shown that, the vibrational

stretching peak due to alcoholic -OH group is different for the different samples. For all these cases a broad nature of stretching frequency due to -OH group is found in the FTIR spectra. Interestingly, broadening nature decreases gradually from TEMPO-MEA-CNC to CNC-80. The intensity of the C-H vibrational band is also different for the different CNCs sample. The vibrational stretching frequency due to carbonyl C=O group is also different for the different CNC-mediated samples. For TEMPO-MEA-CNC, C=O band is found at 1589 cm^{-1}, which is different from other samples and for CNC-80 it is coming at 1675 cm^{-1} in the FTIR spectra. The vibrational stretching band for C-O-C functional group is also found different for different samples. Therefore, it can be attributed from the FTIR spectra studies that, although all CNC mediated samples possess identical functional groups but they are not identical structurally.

Table 4.1 Details of FTIR Spectra (different type of celluloses) Obtained from figure 4.2. Vibrational stretching frequency for different functional groups are presented in table.

Absorption(cm^{-1})	Presence of group	Nature of appearance
3411.49	–OH group	peak is bulgy
about 3000 - 3700	prominent band in alcohols is due to the O-H bond	It appears strong
Above 2800-3500	O-H stretch	carboxylic acids show a very strong band
around 1710	C=O stretch	stake-shaped band
2965.99	carboxylic acid group	strong
3000	C-H stretching	Methyl
1178	anti-symmetric stretching vibrations	C-O-C bridge
1073	C-O stretching	skeletal vibrations
906	glucosidic ring	present in the cellulose.
above 3100-3500	N-H stretch	very strong
around 1710	C=O stretch	stake-shaped

4.1.2 X-Ray Diffraction

XRD of CNC-I prepared from crotalaria junchea using pre-treatment processes mentioned by [10] showed two peaks one for Cellulose–I and another for Cellulose-II while for CNC-II only cellulose-I peak was observed (Figure 4.3). By using the popular formula reported by [52] the

Crystallinity index of the sample was calculated and it was found out to be 80 for CNC-I while for CNC-II it was found to be 75.

$CrI=((I_{crys}-I_{am})/I_{crys})*100$…….(1) [52]

Thus Crystalline properties of CNC-II was found to be less than that of CNC-I as the Crystallinity index (CI) of CNC-I was found to be more than that of CNC-II from Figure 4.3.

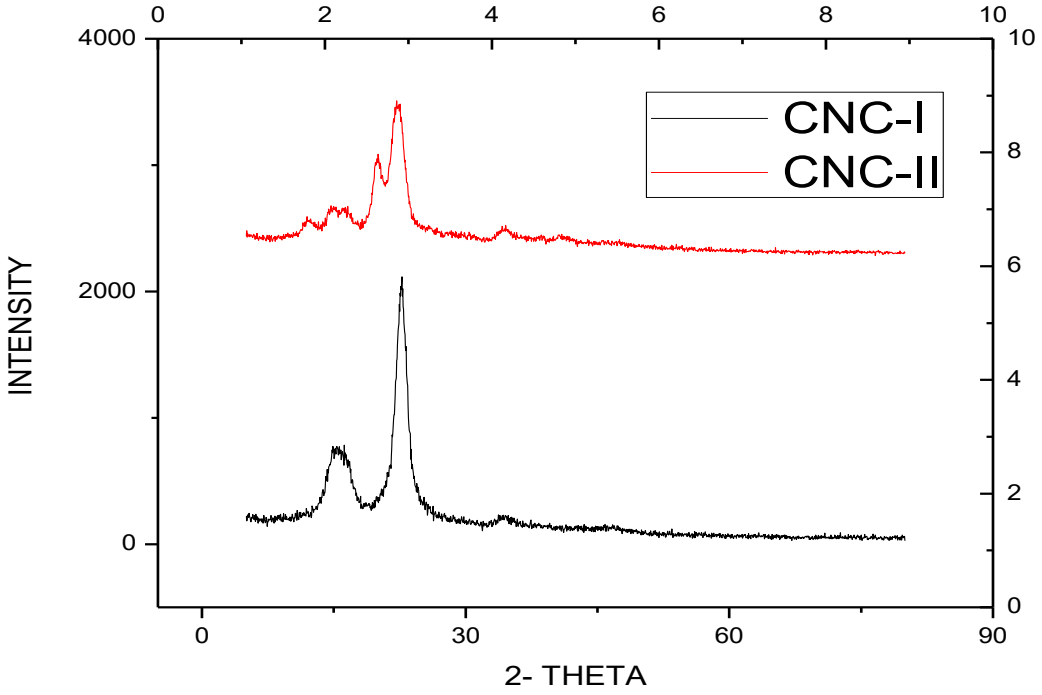

Figure 4.3 XRD Plot of CNC-I and CNC-II

Table 4.2 Crystallinity Index

SAMPLE	CRYSTALLINITY INDEX
CNC	80.9
TEMPO-OXIDISED CNC	77.39

4.1.3 BET Surface Analyser

The BET theory was developed by Stephen Brunauer, Paul Emmett, and Edwrd Teller in 1938. The BET theory was an extension of the Langmuir theory, developed by Irving Langmuir in 1916. The permanent porosity and surface properties of the CNCs materials were investigated by N_2 adsorption-desorption analyses. Nitrogen adsorption/desorption isotherms were conducted using a Quanta chrome Instruments Autosorb 1C BET surface area analyser. Before the analysis the samples were degassed at 193 K for 3 h under high vacuum. The sorption isotherms and pore size distribution curves are shown in Figure 4.4 a and b. The adsorption isotherms of the CNCs materials demonstrated steep nitrogen uptakes in the lower pressure region, suggesting their

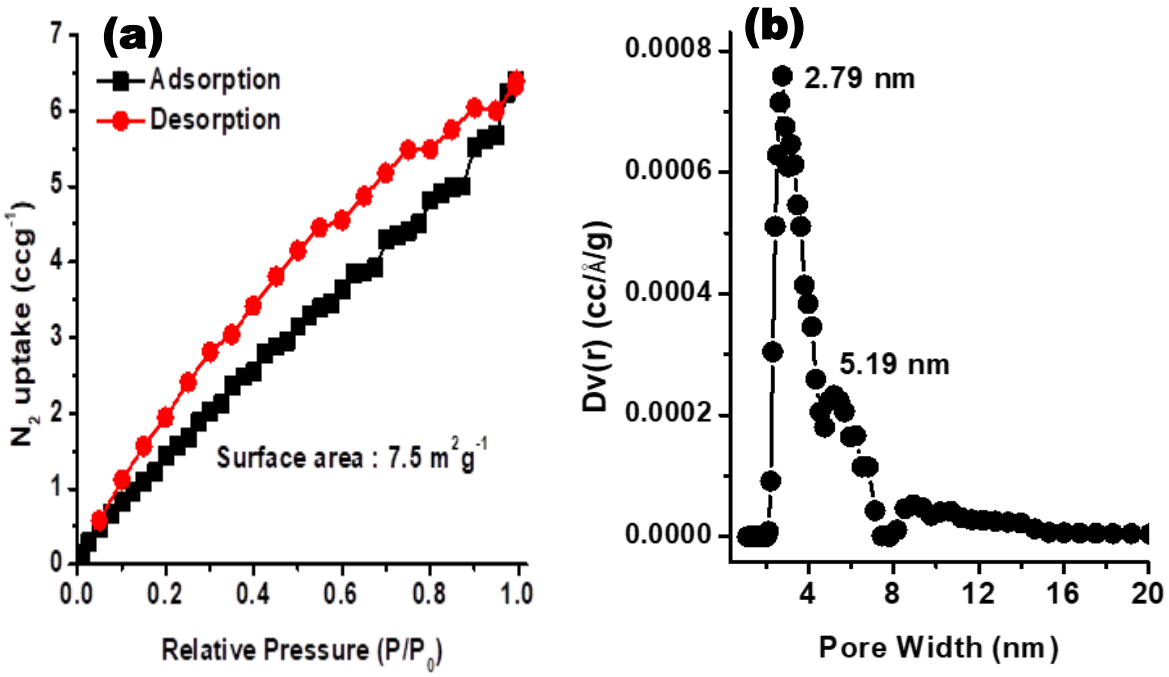

Figure 4.4 (a) Nitrogen adsorption/desorption isotherms of CNC and (b) corresponding non-local density functional theory pore size distributions.

mesoporous nature. The Brunauer–Emmett–Teller (BET) surface area of CNC-I is 7.5 m^2 g^{-1}. The weak peaks corresponding to mesopores is observed in synthesized CNC-I material. The mesoporosity of the materials is probably due to the presence of interparticle voids or cages in the networks.

4.1.4 Scanning Electron Microscope (SEM)

A scanning electron microscope (SEM) is a type of electron microscope that produces images of a sample by scanning it with a focused beam of electrons. The electrons interact with atoms in the sample, producing various signals that contain information about the sample's surface topography and composition. The electron beam is generally scan in a raster scan pattern and the beam's position is combined with the detected signal to produce an image. SEM is achieved resolution better than one nanometre. Specimens can be observed in high vacuum, in low vacuum, in weight condition (in environmental SEM), and at a wide range of cryogenic or elevated temperature. The most common SEM mode is detection of secondary electron emitted by atoms of excited by the electron beam. The number of secondary electron that can be detected

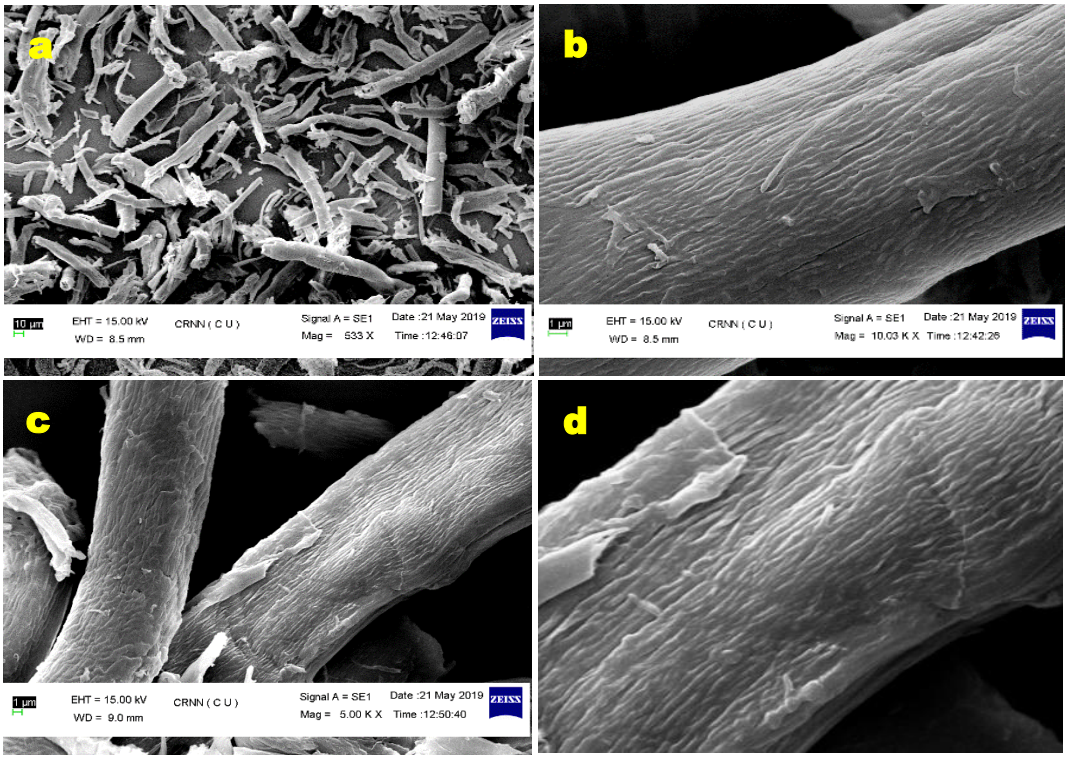

Figure:4.5 SEM images of CNC

depends among other things, on specimen topography. By scanning the sample, a collecting the secondary electrons that are emitted using a special detector, an image displaying the topography of the surface is created. SEM images of the sample were observed through a ZEISS SEM instrument (Model: ZEISS EVO-MA10) operating at 15 kV after Platinum coating. From the

figure 4.5 it has been observed that a number of micro-tubes of CNC-I (figure 4.5 a) are consist of nanotubes (figure 4.5 b, c, d) which are connected side by side in parallelly manner.

4.1.5 Determination of degree of sulfation

Degree of sulfation of the prepared CNC samples were determined by performing the conductometric titration, by suspending the CNC's in 0.001M NaCl solution and titrated against 0.01N NaOH solution. [53], and the calculated value for CNC- I was found to be 0.34 m eqv/gm, which confirmed higher degree of sulfation compared to CNC-II. The degree of sulfation was found to be 0.067 m eqv/gm for CNC-II which was quite low probably due to the lower reaction time as well as a relatively inefficient pretreatment.

From these characterizations it was realized that CNC-I is superior in quality compared to CNC-II which prompted to examine the adsorption characteristics of CNC-I

4.2.1 Adsorption Studies by CNC-I

The adsorption of methylene blue using CNC-I was designed using central composite design through Design expert software.

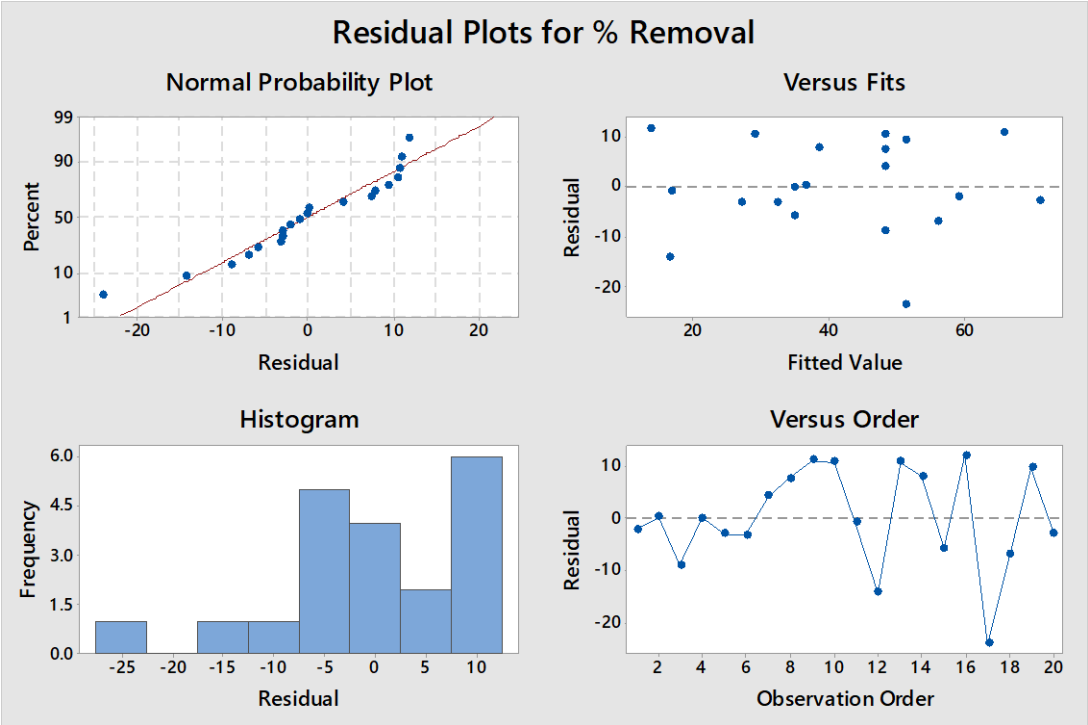

Figure 4.6 Residual plots for experimental data vs stimulated data

4.2.2 Residual plots for percentage removal of Methylene Blue

The residual plot of the adsorption data revealed that simulated data are in coherence with the experimental results as depicted in Fig. 4.6.

- **Effect of pH**

The effect of pH values on the adsorption capacity of CNC was shown in Figure 4.7. The amount of MB adsorption was significant increased when the surrounding pH varied from 5.0 to 10.0, It has been reported that the higher pH can cause the ionization of carboxyl acid groups and thus increase the interactions between negatively charged groups in materials and dye cations. Moreover, at higher pH, increased ionized groups cause to generate electrostatic repulsion forces among the adjacent ionized groups of polymer networks. This produces an expansion network like ultrastructure of the hydrogels, which may also result in an increase of MB adsorption. [54]

- **Effect of solute concentration**

Figure 4.7 shows the effect of solute concentration on the removal of MB using CNC. The decomposition of dye decreased with the increasing dye concentration, at initial dye concentration is lower, therefore decomposition of dye decreased with decreasing initial dye concentration. At 75 ppm the decomposition of dye capacity was higher than other solute concentration. Although the percent adsorption decreased with increase in initial dye concentration and time, which is quite clear from the trend of percent adsorption, the actual amount of dye adsorbed per unit mass of adsorbent increased with increase in dye concentration in the test solution. [55]

- **Effect of adsorbate loading**

Figure 4.7 shows the effect of bio adsorbent dosage on the dye removal efficiency by contacting 50 mL of dye solution with an initial concentration of 1gm L−1 at 25°C for 48 hours. For optimum loading, 50 ppm solution of MB was used along with different loading ranging from 1g/L to 4g/L. Figure shows the effect of CNC loading on percentage degradation of MB after 48 hours, the percentage of dye degradation increased from 29.00 % to 52.17 %, when the loading was increased from 1 g/L to 2.5 g/L, but it decreased to 34.82% on further increasing the loading. This can be explained by the fact, dye removal efficiency increased dramatically with increasing

% Removal = -60 + 29.9 Loading (g/L) - 0.69 Concentration of MB (ppm) + 26.5 pH - 2.71 Loading (g/L) * Loading (g/L) + 0.00217 Concentration of MB (ppm) *Concentration of MB (ppm) - 1.805 pH*pH - 0.090 Loading (g/L) *Concentration of MB (ppm) - 0.12 Loading (g/L)*pH+ 0.0239 Concentration of MB (ppm)*pH

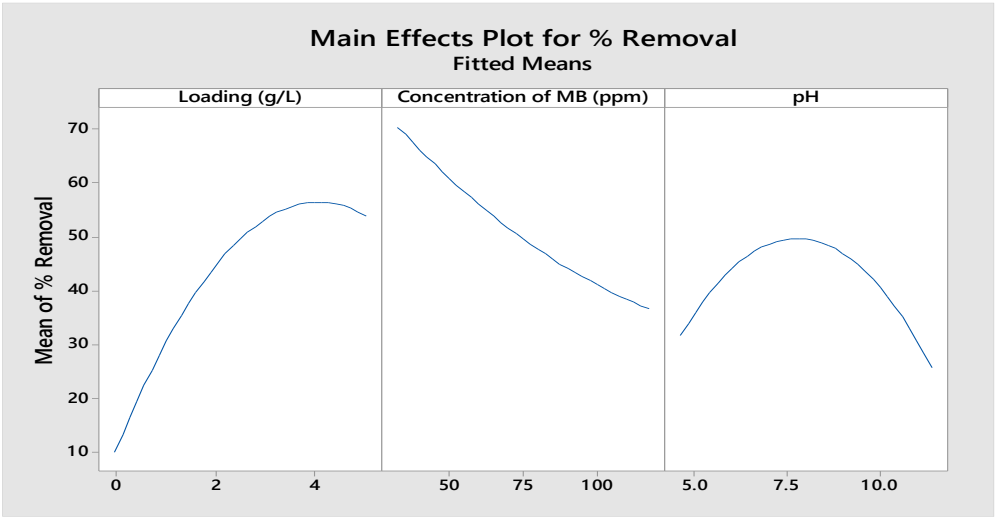

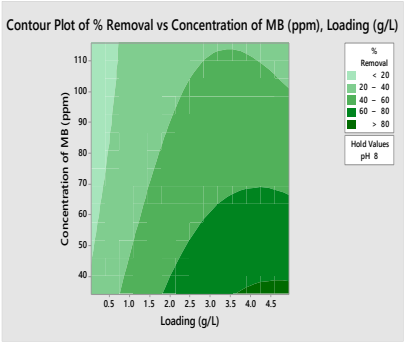

% Removal vs Conc. of MB

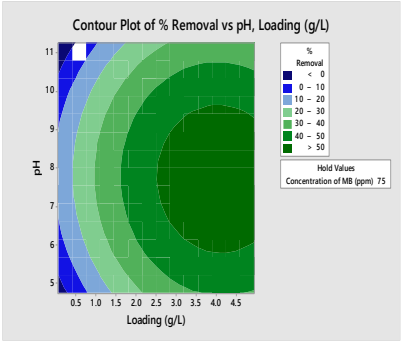

% Removal vs pH

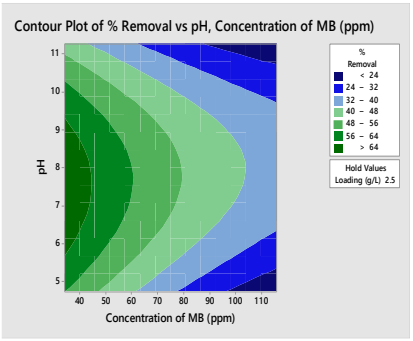

% Removal vs pH Conc. of MB

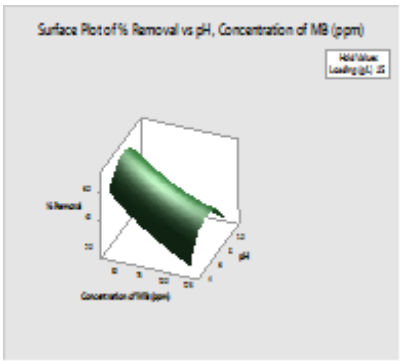

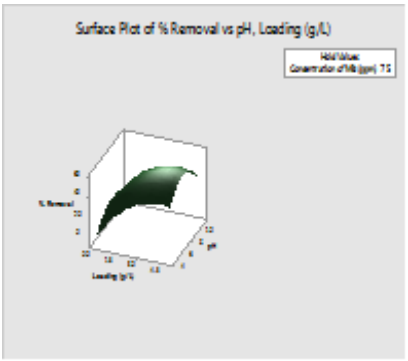

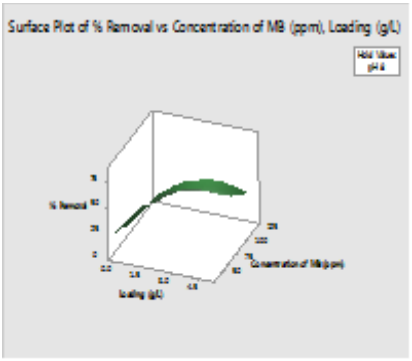

Figure 4.7 Main effects plot and surface plots of %removal of MB as a function of loading (g/l), concentration (ppm) and pH of the solution.

the bio adsorbent dosage, which was due to the increase of available adsorption sites in cellulose-based bio adsorbents. However, on further addition of adsorbate, the solution became turbid and adsorbate could not penetrate through solution. [56]

❖ Response surface methodology

Response surface methodology was employed for the adsorption of methylene blue (MB) by CNC-I nanoparticles. The process parameters for RSM were loading of CNCs (g/l), concentration of MB (ppm) and pH of the solution while removal efficiency being the response variable. A total of 20 adsorption experiments were carried out in order to optimize the parameters. The results revealed the following regression equation. It can also be visualized by main effects plot and surface plots that highest % removal of MB occurred at an optimal pH of 8, loading 4g/l and lower MB concentration. A maximum of 70% removal was achieved within 1h of contact time (Figure 4.7).

4.2.3 Effect of Time on Adsorption Capacity

10 different times (5min, 10min, 20min, 30min, 45min, 1hr, 2hr, 4hr, 20h, 24h) were studied with dye concentration of 10 ppm and loading of 1 g/L. Figure shows that the effect of activation time on the adsorption capacity of the prepared CNC. With increase in activation time the adsorption capacity also increased. Here the highest adsorption capacity is 58%.

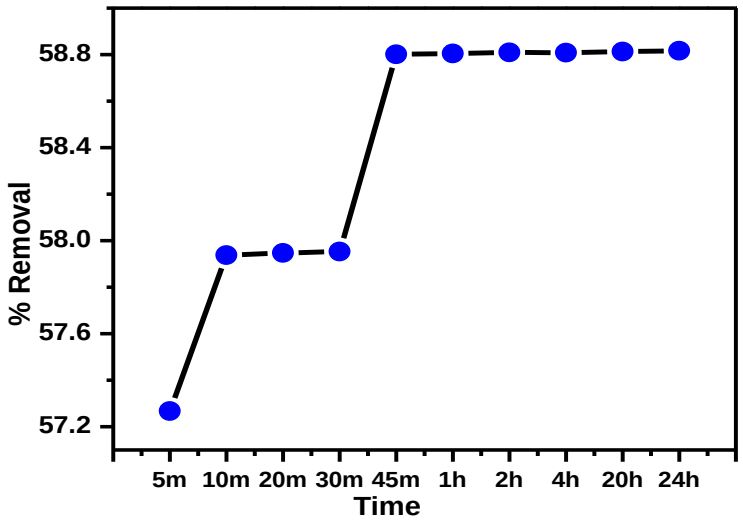

Figure 4.8 Effect of activation time on the adsorption of Methylene Blue onto prepared CNC at 25^0

4.2.4 Different type of adsorbate for adsorption of Methylene Blue

5 different samples (tempo CNC, PM-4 tempo CNC, sonicated CNC, bacterial tempo CNC, amine CNC) were studied with dye concentration of 50 PPM and loading of 1 gm/L. Figure 4.13 shows effect of the adsorption of Methylene Blue using different CNC-mediated sample. The figure suggests bacterial tempo CNC showed better adsorption than others.

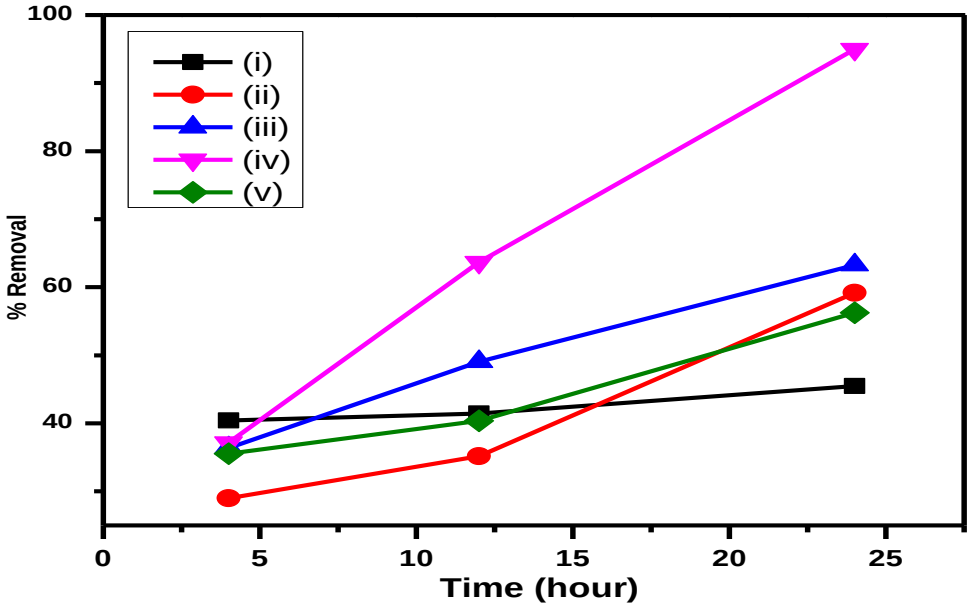

Figure 4.9 (i) Tempo CNC; (ii) PM-4 tempo CNC; (iii) Sonicated CNC; (iv) Bacterial tempo CNC; (v) Amine CNC

4.3 Adsorption of Malachite Green using CNC

4.3.1 Effect of Time on Adsorption Capacity

6 different times (5min, 10min, 1hr, 4h, 20h, 24h) were studied with Malachite Green dye concentration of 100 ppm and loading of 1 g/L. Figure shows that the effect of activation time on the adsorption capacity of the prepared CNC. With increase in activation time the adsorption capacity also increased. Here the highest adsorption capacity is 62%.

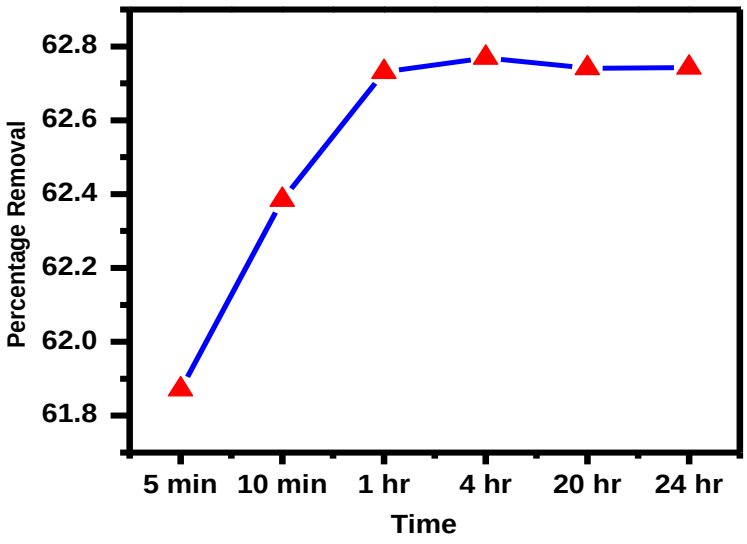

Figure 4.10 Effect of activation time on the adsorption of Malachite Green onto prepared CNC at 25^0

4.3.2 Different type of adsorbate for adsorption of Malachite green

5 different samples (tempo CNC, PM-4 tempo CNC, sonicated CNC, bacterial tempo CNC, amine CNC) were studied with dye concentration of 10 PPM and loading of 1 gm/L. Figure 4.11 shows effect of the adsorption of Malachite green using different CNC-mediated sample. The figure suggests tempo CNC showed better adsorption than others adsorbents.

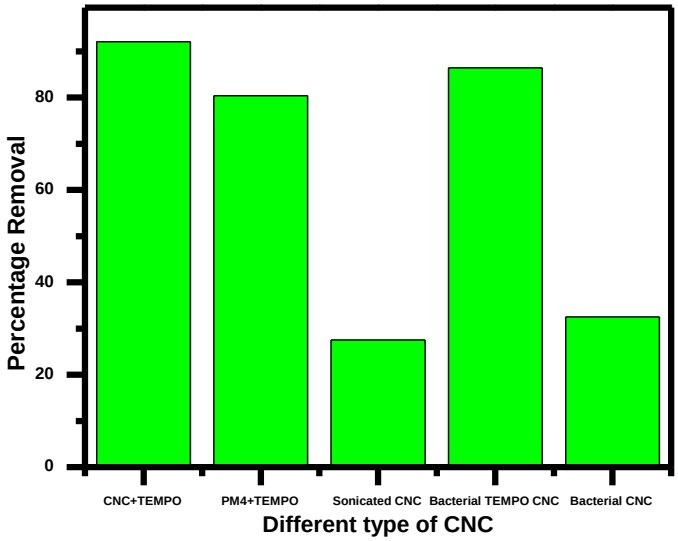

Figure 4.11 Adsorption of Malachite green using different types of CNC

4.4 Comparison between the percentage removal of Malachite green and Methylene blue solution

5 different samples (tempo CNC, PM-4 tempo CNC, sonicated CNC, bacterial tempo CNC, bacterial CNC) were studied with dye concentration of 10 PPM, loading of 1 gm/L and the reaction time of 24 hours. Figure 4.12 shows comparison between the percentage of removal of both Methylene Blue and Malachite Green solution using different CNC-mediated sample. The figure suggests for tempo CNC give better adsorption performance for the removal of Malachite green, PM-4 tempo CNC give better adsorption performance in Malachite green solution, Sonicated CNC give better adsorption performance in Methylene blue solution, Bacterial tempo CNC give better adsorption performance in Methylene blue solution and Bacterial CNC give better adsorption performance in Methylene blue solution. Tempo-mediated bacterial CNC showed highest adsorption capacity for MG while tempo mediated CNC showed highest removal for MB. It was also realized from the below figure that tempo mediated samples exhibited better removal efficiencies of MG while bacterial CNC both pristine and tempo mediated showed high removal for MB. This was probably due to presence of carboxylic acid groups in tempo mediated CNCs which interacted with MG resulting higher removal percentages.

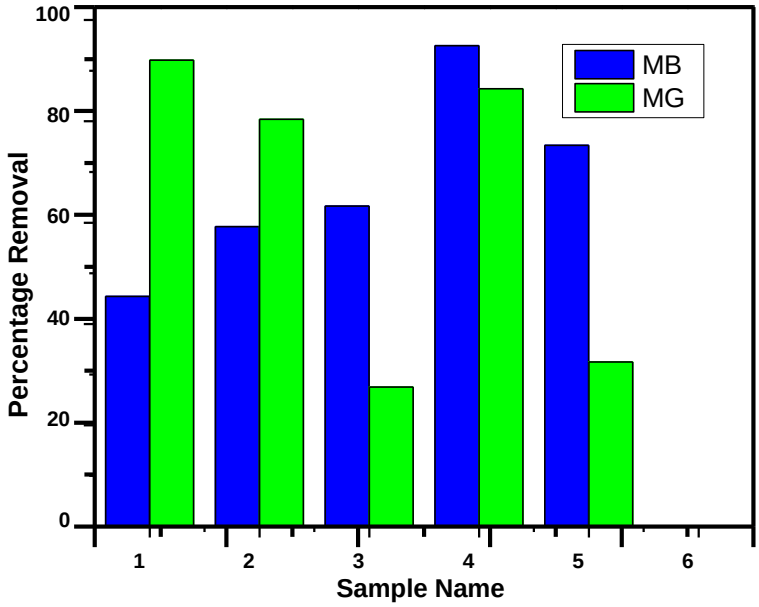

Figure 4.12 Comparison between Methylene Blue & Malachite Green using different adsorbent (1) Tempo CNC; (2) PM-4 tempo CNC; (3) Sonicated CNC; (4) Bacterial tempo CNC; (5) Bacterial CNC.

From a comparison studies (dye adsorption) by taking five different CNCs materials using methylene blue and malachite green dye it has been found that, adsorption performance (adsorption of methylene blue) of a commercial bacterial CNCs is better than other. On the other hand, adsorption performance (adsorption of malachite green) of surface modified CNCs is better than normal CNCs.

In future, better surface modification of the CNCs will be done for better adsorption of toxic materials, which could be better applicable as commercial material and economically viable.

CHAPTER-V

5.1 Conclusion

Nanocelluloses (CNC-I and CNC-II) were successfully prepared by acid hydrolysis of the pre-treatment residues obtained from Crotalaria juncea. The characterization of CNCs have been done by FTIR, Powder XRD, SEM and BET studies. From FTIR study, it has been found that, CNC-I and CNC-II exhibit different stretching vibrational peaks due presence of different functional groups in CNCs, indicating CNC-I and CNC-II are structurally not identical. From powder XRD study it is attributed that, the CNC-I and CNC-II exhibit a number of crystalline peaks, but packing pattern of CNC-I and CNC-II are different. From SEM images, it is visualized that, a number of micro-tubes of CNC-I which are consisting of nanotubes are connected side by side in parallelly manner. The adsorption isotherms of the CNCs materials demonstrated steep nitrogen uptakes in the lower pressure region, suggesting their mesoporous nature. The mesoporosity of the materials is probably due to the presence of interparticle voids or cages in the networks. The surface area of CNC-I has been calculated from BET which is found to be 7.5 m^2 g^{-1}. The adsorption of methylene blue by CNC-I experiment has been performed at varying pH from 5.0 to 10, suggesting at higher pH ionization of carboxyl acid groups and thus increase the interactions between negatively charged groups present in CNCs and dye cations. The adsorption of dye by CNCs is found to be better at the higher concentration of dye. The adsorption capacity of dye by CNCs is increased with increasing of activation times and it has been found that the highest capacity of adsorption is 58 % at 20 hours. From a comparison studies (dye adsorption) by taking five different CNCs materials using methylene blue and malachite green dye it has been found that, adsorption performance (adsorption of methylene blue) of a commercial bacterial CNCs is better than other. On the other hand, adsorption performance (adsorption of malachite green) of surface modified CNCs is better than normal CNCs.

5.2 Future prospects of the work

- Methylene blue and Malachite green were selected as the model dyes for all adsorption experiments. Studies can be carried out with other organic substances and heavy metals to investigate whether the prepared material adsorbs other substances as efficiently as it degrades Methylene blue and Malachite green.
- In this study maximum concentration of 100 ppm was taken. To understand the processes better experiments can be performed at higher concentration to see the effects on dye removal efficiency.
- Chemical modification of prepared cellulose will be done for high adsorption capacity, which enhance the performance of material.
- The reusability study of material has to be also performed.

REFFERENCES

[1] H. Voisin, L. Bergström, P. Liu, and A. Mathew, "Nanocellulose-Based Materials for Water Purification," *Nanomaterials*, vol. 7, no. 3, p. 57, 2017.

[2] T. Suopajarvi, *Functionalized nanocelluloses in wastewater treatment applications*. 2015.

[3] N. Mohammed, N. Grishkewich, and K. C. Tam, "Cellulose nanomaterials: promising sustainable nanomaterials for application in water/wastewater treatment processes," *Environ. Sci. Nano*, vol. 5, no. 3, pp. 623–658, 2018.

[4] H. Liang and X. Hu, "A quick review of the applications of nano crystalline cellulose in wastewater treatment," vol. 1, no. 4, pp. 199–204, 2016.

[5] R. J. Moon, A. Martini, J. Nairn, J. Simonsen, and J. Youngblood, *Cellulose nanomaterials review: structure, properties and nanocomposites*, vol. 40, no. 7. 2011.

[6] D. Puglia, J. Biagiotti, and J. Kenny, "A review on natural fibre-based composites—part II: application of natural reinforcements in composite materials for automotive industry," *J. Nat. Fibers*, vol. 1, no. 3, pp. 23–65, 2004.

[7] F. Horii, "Structure of cellulose: recent developments in its

characterization," in *Wood and Cellulosic Chemistry (2nd Edition)*, 2001, pp. 83–107.

[8] L. Brinchi, F. Cotana, E. Fortunati, and J. M. Kenny, "Production of nanocrystalline cellulose from lignocellulosic biomass: Technology and applications," *Carbohydr. Polym.*, vol. 94, no. 1, pp. 154–169, 2013.

[9] T. Zimmermann, E. Pöhler, and P. Schwaller, "Mechanical and morphological properties of cellulose fibril reinforced nanocomposites," *Adv. Eng. Mater.*, vol. 7, no. 12, pp. 1156–1161, 2005.

[10] A. Mandal and D. Chakrabarty, "Isolation of nanocellulose from waste sugarcane bagasse (SCB) and its characterization," *Carbohydr. Polym.*, vol. 86, no. 3, pp. 1291–1299, 2011.

[11] M. A. S. Azizi Samir, F. Alloin, and A. Dufresne, "Review of recent research into cellulosic whiskers, their properties and their application in nanocomposite field," *Biomacromolecules*, vol. 6, no. 2, pp. 612–626, 2005.

[12] G. Siqueira, J. Bras, and A. Dufresne, "Cellulosic bionanocomposites: A review of preparation, properties and applications," *Polymers*, vol. 2, no. 4. pp. 728–765, 2010.

[13] A. Smook, G, *Handbook for Pulp and Paper Technologists*. 1989.

[14] B. M. Cherian, A. L. Leão, S. F. de Souza, S. Thomas, L. A. Pothan, and M. Kottaisamy, “Isolation of nanocellulose from pineapple leaf fibres by steam explosion,” *Carbohydr. Polym.*, vol. 81, no. 3, pp. 720–725, 2010.

[15] B. G. Rånby, “The Colloidal Properties of Cellulose Micelles,” *Discuss. Faraday Soc.*, vol. 11, no. 111, pp. 158–164, 1951.

[16] X. U. E. M. I. N. Dong, “Effect of microcrystallite preparation conditions on the formation of colloid crystals of cellulose,” *Cellulose*, vol. 5, pp. 19–32, 1998.

[17] S. Hokkanen, E. Repo, L. J. Westholm, S. Lou, T. Sainio, and M. Sillanpää, “Adsorption of Ni2+, Cd2+, PO43-and NO3-from aqueous solutions by nanostructured microfibrillated cellulose modified with carbonated hydroxyapatite,” *Chem. Eng. J.*, vol. 252, pp. 64–74, 2014.

[18] H. Sehaqui *et al.*, “Enhancing adsorption of heavy metal ions onto biobased nanofibers from waste pulp residues for application in wastewater treatment,” *Cellulose*, vol. 21, no. 4, pp. 2831–2844, 2014.

[19] S. Srivastava, A. Kardam, and K. R. Raj, “Nanotech reinforcement onto cellulosic fibers: Green remediation of toxic metals,” *Int. J. Green Nanotechnol. Biomed.*, vol. 4, no. 1, pp. 46–53, 2012.

[20] M. A. Mohamed *et al.*, “An overview on cellulose-based material in tailoring bio-hybrid nanostructured photocatalysts for water treatment and renewable energy applications,” *Int. J. Biol. Macromol.*, vol. 103, pp. 1232–1256, 2017.

[21] L. Jin, W. Li, Q. Xu, and Q. Sun, “Amino-functionalized nanocrystalline cellulose as an adsorbent for anionic dyes,” *Cellulose*, vol. 22, no. 4, pp. 2443–2456, 2015.

[22] A. M. Donia, A. A. Atia, and F. I. Abouzayed, “Preparation and characterization of nano-magnetic cellulose with fast kinetic properties towards the adsorption of some metal ions,” *Chem. Eng. J.*, vol. 191, pp. 22–30, 2012.

[23] C. Guo, L. Zhou, and J. Lv, “Effects of expandable graphite and modified ammonium polyphosphate on the flame-retardant and mechanical properties of wood flour-polypropylene composites,” *Polym. Polym. Compos.*, vol. 21, no. 7, pp. 449–456, 2013.

[24] M. L. Metzker, “Sequencing technologies the next generation,” *Nature Reviews Genetics*, vol. 11, no. 1. pp. 31–46, 2010.

[25] K. Xie, W. Zhao, and X. He, “Adsorption properties of nano-cellulose hybrid containing polyhedral oligomeric silsesquioxane and removal of reactive dyes from aqueous solution,” *Carbohydr. Polym.*, vol. 83, no. 4, pp. 1516–1520, 2011.

[26] L. M. Zhao *et al.*, “Preparation and application of chitosan nanoparticles and nanofibers,” *Brazilian Journal of Chemical Engineering*, vol. 28, no. 3. pp. 353–362, 2011.

[27] J. Araki, M. Wada, and S. Kuga, “Steric stabilization of a cellulose microcrystal suspension by poly(ethylene glycol) grafting,” *Langmuir*, vol. 17, no. 1, pp. 21–27, 2001.

[28] F. Kimura, T. Kimura, M. Tamura, A. Hirai, M. Ikuno, and F. Horii, “Magnetic alignment of the chiral nematic phase of a cellulose microfibril suspension,” *Langmuir*, vol. 21, no. 5, pp. 2034–2037, 2005.

[29] J.-F. Revol, “On the cross-sectional shape of cellulose crystallites in Valonia ventricosa,” *Carbohydr. Polym.*, vol. 2, no. 2, pp. 123–134, Jan. 1982.

[30] L. Pranger and R. Tannenbaum, “Biobased Nanocomposites Prepared by In Situ Polymerization of Furfuryl Alcohol with Cellulose Whiskers or Montmorillonite Clay Biobased Nanocomposites Prepared by In Situ Polymerization of Furfuryl Alcohol with Cellulose Whiskers or Montmorillonite Clay,” pp. 8682–8687, 2008.

[31] X. Yang and E. D. Cranston, “Chemically cross-linked cellulose nanocrystal aerogels with shape recovery and superabsorbent properties,” *Chem. Mater.*, vol. 26, no. 20, pp. 6016–6025, 2014.

[32] Q. Li, J. Zhou, and L. Zhang, “Structure and properties of the nanocomposite films of chitosan reinforced with cellulose whiskers,” *J. Polym. Sci. Part B Polym. Phys.*, vol. 47, no. 11, pp. 1069–1077, 2009.

[33] Y. Huang and D. R. Paul, “Effect of MolecularWeight and Temperature on Physical Aging of ThinGlassy Poly(2,6-dimethyl-1,4-phenylene oxide) Films,” *J. Polym. Sci. Part B Polym. Phys.*, vol. 45, no. April, pp. 1390–1398, 2007.

[34] S. Beck-Candanedo, M. Roman, and D. G. Gray, “Effect of reaction conditions on the properties and behavior of wood cellulose nanocrystal suspensions,” *Biomacromolecules*, vol. 6, no. 2, pp. 1048–1054, 2005.

[35] A. Dufresne and M. R. Vignon, “Improvement of starch film performances using cellulose microfibrils,” *Macromolecules*, vol. 31, no. 8, pp. 2693–2696, 1998.

[36] P. Lu and Y. Lo Hsieh, “Preparation and characterization of cellulose nanocrystals from rice straw,” *Carbohydr. Polym.*, vol. 87, no. 1, pp. 564–573, 2012.

[37] M. F. Rosa *et al.*, “Cellulose nanowhiskers from coconut husk fibers: Effect of preparation conditions on their thermal and morphological behavior,” *Carbohydr. Polym.*, vol. 81, no. 1, pp. 83–92, 2010.

[38] W. H. Danial, Z. Abdul Majid, M. N. Mohd Muhid, S. Triwahyono, M. B. Bakar, and Z. Ramli, “The reuse of wastepaper for the extraction of cellulose nanocrystals,” *Carbohydr. Polym.*, vol. 118, pp. 165–169, 2015.

[39] M. S. Peresin, Y. Habibi, J. O. Zoppe, J. J. Pawlak, and O. J. Rojas, “Nanofiber Composites of Polyvinyl Alcohol and Cellulose Nanocrystals: Manufacture and Characterisation,” *Biomacromolecules*, vol. 11, no. 3, pp. 674–681, 2010.

[40] N. L. Garcia de Rodriguez, W. Thielemans, and A. Dufresne, “Sisal cellulose whiskers reinforced polyvinyl acetate nanocomposites,” *Cellulose*, vol. 13, no. 3, pp. 261–270, 2006.

[41] J. I. Morán, V. A. Alvarez, V. P. Cyras, and A. Vázquez, “Extraction of cellulose and preparation of nanocellulose from sisal fibers,” *Cellulose*, vol. 15, no. 1, pp. 149–159, 2008.

[42] F. Luzi *et al.*, “Optimized extraction of cellulose nanocrystals from pristine and carded hemp fibres,” *Ind. Crops Prod.*, vol. 56, pp. 175–186, 2014.

[43] N. A. Rosli, I. Ahmad, and I. Abdullah, “Isolation and characterization of cellulose nanocrystals from agave angustifolia fibre,” *BioResources*, vol. 8, no. 2, pp. 1893–1908, 2013.

[44] J. Giménez, M. Martínez, J. de Pablo, M. Rovira, and L. Duro,

"Arsenic sorption onto natural hematite, magnetite, and goethite," *J. Hazard. Mater.*, 2007.

[45] S. Hokkanen, E. Repo, and M. Sillanpää, "Removal of heavy metals from aqueous solutions by succinic anhydride modified mercerized nanocellulose," *Chem. Eng. J.*, vol. 223, pp. 40–47, 2013.

[46] S. Luther, N. Borgfeld, J. Kim, and J. G. Parsons, "Removal of arsenic from aqueous solution: A study of the effects of pH and interfering ions using iron oxide nanomaterials," *Microchem. J.*, vol. 101, pp. 30–36, 2012.

[47] P. Xia, B. Zhu, J. Yu, S. Cao, and M. Jaroniec, "Ultra-thin nanosheet assemblies of graphitic carbon nitride for enhanced photocatalytic CO_2 reduction," *J. Mater. Chem. A*, vol. 5, no. 7, pp. 3230–3238, 2017.

[48] N. Lin, C. Bruzzese, and A. Dufresne, "TEMPO-oxidized nanocellulose participating as crosslinking aid for alginate-based sponges," *ACS Appl. Mater. Interfaces*, vol. 4, no. 9, pp. 4948–4959, 2012.

[49] A. Dufresne, "Polysaccharide nano crystal reinforced nanocomposites," *Can. J. Chem.*, vol. 86, no. 6, pp. 484–494, 2008.

[50] M. K. Nacos *et al.*, "Kenaf xylan - A source of biologically active

acidic oligosaccharides," *Carbohydr. Polym.*, vol. 66, no. 1, pp. 126–134, 2006.

[51] H. P. S. A. Khalil, H. Ismail, H. D. Rozman, and M. N. Ahmad, "Effect of acetylation on interfacial shear strength between plant fibres and various matrices," *Eur. Polym. J.*, vol. 37, no. 5, pp. 1037–1045, 2001.

[52] S. Baksi *et al.*, "Valorization of Lignocellulosic Waste (Crotalaria juncea) Using Alkaline Peroxide Pretreatment under Different Process Conditions: An Optimization Study on Separation of Lignin, Cellulose, and Hemicellulose," *J. Nat. Fibers*, vol. 0478, pp. 1–15, 2018.

[53] F. Jiang, A. R. Esker, and M. Roman, "Acid-catalyzed and solvolytic desulfation of H2SO 4-hydrolyzed cellulose nanocrystals," *Langmuir*, vol. 26, no. 23, pp. 17919–17925, 2010.

[54] M. T. A. M. Ende and N. A. Peppas, "Transport of Ionizable Drugs and Proteins in Crosslinked Poly(acrylic acid) and Poly(acry1ic acid-co-2-hydroxyethyl methacrylate) Hydrogels.," vol. 59, pp. 1–13, 2002.

[55] R. Malik, D. S. Ramteke, and S. R. Wate, "Adsorption of malachite green on groundnut shell waste based powdered activated carbon," *Waste Manag.*, vol. 27, no. 9, pp. 1129–1138, 2007.

[56] H. Tang, W. Zhou, and L. Zhang, “Adsorption isotherms and kinetics studies of malachite green on chitin hydrogels,” *J. Hazard. Mater.*, vol. 209–210, pp. 218–225, 2012.